

On the integral variation map of isolated plane curve singularities

Pablo Portilla Cuadrado* Baldur Sigurðsson†

December 5, 2025

Abstract

The integral variation map and algebraic monodromy of isolated plane curve singularities are important homological invariants of the singularity which are still far from being completely understood. This work provides effective ways of computing them with respect to an explicit geometric basis of the homology.

For any given topological type of plane curve singularity, we construct an analytic model of it, along with a vector field on our version of its A'Campo space. This vector field is tangent to the Milnor fibers at radius zero and the union of the stable manifolds of their singularities yields a spine of each fiber, which can be described explicitly. This is very much inspired by a recent work of the authors.

Our first main contribution is the algorithmic computation of the algebraic monodromy and integral variation map as matrices with explicit bases for any Milnor fiber in the Milnor fibration, not merely congruence classes. For our second contribution, we introduce gyrographs which are graphs equipped with angular data and rational weights. We prove that the invariant spine naturally carries a gyrograph structure where the weights are given by the Hironaka numbers, and that this structure recovers the geometric monodromy as a homotopy class, as well as the integral variation map. This provides a combinatorial framework for computation by hand. Our methods are further implemented in a publicly available computer program written in Python.

Contents

1	Introduction	2
2	Preparation	5
2.1	Initial data	5
3	Construction of an analytic model	9
3.1	Analytic charts	9
3.2	A regular sequence	10
3.3	Local expressions for f	10
3.4	Description of the invariant Milnor fibration	12
3.5	Description of the flow	16
4	The spine	20

*The first author is supported by RYC2022-035158-I, funded by MCIN/AEI/10.13039/501100011033 and by the FSE+

†The second author was partly supported by Contratos María Zambrano para la atracción de talento internacional at Universidad Complutense de Madrid and Universidad Politécnica de Madrid and the Spanish grant of MCIN (PID2020-114750GB-C32/AEI/10.13039/501100011033).

5	Dynamics of the vector field	21
5.1	Generic angles	23
5.2	The set of non-generic angles	24
6	Algebraic monodromy and variation	25
6.1	A chain complex	25
6.2	The action on the chain complex	29
6.3	Action on homology	33
7	Description of the variation operator	33
7.1	V on the chain complex	33
7.2	Var on homology	34
8	Gyrographs	34
8.1	A general construction	35
8.2	The invariant spine as a gyrograph	36
8.3	An example with two Puiseux-pairs	38
9	Software implementation	42
9.1	Usage	42
9.2	Example	44

1 Introduction

The topological type of an isolated plane curve singularity $(C, 0) \subset (\mathbb{C}^2, 0)$, defined by a germ $f \in \mathbb{C}\{x, y\}$ can be encoded in the minimal resolution graph. The topological information can be also fully recovered from the Milnor fibration, that is, from the locally trivial fibration

$$f^{-1}(\partial D_\delta) \cap B_\varepsilon \rightarrow \partial D_\delta$$

given by the restriction of f to the preimage of a small circle intersected with a small enough sphere, with $0 < \delta \ll \varepsilon$. Its fiber F is called the Milnor fiber, and its characteristic mapping class

$$G : F \rightarrow F$$

is called the *geometric monodromy*. Its induced action at the homological level is the algebraic monodromy associated with the Milnor fibration

$$G_1 : H_1(F; \mathbb{Z}) \rightarrow H_1(F; \mathbb{Z}).$$

The singularity being isolated allows one to consider a well defined geometric monodromy which acts by the identity on the boundary ∂F on the Milnor fiber which, in turn, allows for the definition of the variation map with integral coefficients

$$\begin{aligned} \text{Var} : H_1(F, \partial F; \mathbb{Z}) &\rightarrow H_1(F; \mathbb{Z}) \\ [a] &\mapsto [G(a) - a] \end{aligned}$$

where a is any relative cycle representing $[a]$.

Both the algebraic monodromy and the variation map are homological algebraic invariants of the embedded topological type of a plane curve. The variation map is equivalent to the Seifert form, and it determines the algebraic monodromy. There does not exist a satisfactory classification for these algebraic objects. Indeed, there is no good generalization of the (generalized) Jordan canonical form of a linear endomorphism on a finitely generated free \mathbb{Z} -module, nor is

there any classification of integral bilinear (and non-symmetric) forms which encode the variation map. This work builds towards the objective of better understanding these objects.

Results in this direction include Selling-reduction [Sel73] which was used by Kaenders to prove that the Seifert form determines the intersection numbers between branches of a curve singularity [Kae96]. Also, explicit description of the Seifert form is obtained in [EN85] for a class of links including algebraic ones, as well as by A'Campo [A'C75b, A'C75c, A'C99, A'C98] and Gusein-Zade [GZ74] using divides.

It is known that the algebraic monodromy determines the number of branches, and that in the case of one branch, the algebraic monodromy, in fact, its characteristic polynomial, determines its topological type fully. This is no longer the case for two or more branches.

Examples of pairs of plane curve singularities having the same algebraic monodromy but distinct topological types, are given in [Gri74], using rational coefficients, and in [MW86] using integral coefficients. In [dB91], du Bois and Michel describe pairs of plane curves which are topologically distinct, but have the same Seifert form. In particular, the integral variation map does not distinguish them. Deep results in the direction of classifying these homological invariants include [MW86, MW84, DBR07, DBM92].

In order to investigate these homological invariants of a plane curve singularity, the algebraic monodromy and the variation map, we construct explicitly a suitable analytic model of the topological type, as well as a spine in its *invariant A'Campo space*. In [PS25b] we already constructed a spine on the Milnor fibers at radius 0 as the union of the stable manifolds associated with a suitable vector field that arises as a limit-rescaled version of the complex gradient of f . The spine in this work is a combination of A'Campo's classical construction of the Milnor fibration at radius zero by real oriented blow up, and interpolating pieces described in [A'C75a], and our work [PS25b]. Here *invariant* means collapsing certain disks in each invariant Milnor fiber at radius zero. The *invariant spine* in this realization of the Milnor fibration consists of an embedded graph in each Milnor fiber. Vertices and edges of this graph are singularities and trajectories of a specific vector field on the invariant Milnor fiber which is similar to that obtained in [PS25b] but slightly modified for computational convenience. This way we get to one of the *main contributions* of the present work: for an arbitrary topological type, we compute explicitly the action of the monodromy of the chain complex associated with a finite graph, as well as a map from the dual chain complex which represents the variation map, with integral coefficients. Our methods are effective and produce, not just congruence classes of matrices but an explicit description of the basis in which these matrices are computed.

Our methods differ from the existing literature in that the calculation of integral matrices representing the algebraic monodromy and variation map are done at the level of the chain complex, obtained by representing the Milnor fiber as a handle body, with $\mu + m_0 - 1$ handles of index 1, and m_0 handles of index zero, where m_0 is the multiplicity. Handle body decompositions of this type, and reductions of them by handle cancellations, have appeared in the algebraic and topological study of hypersurface singularities in [Trá75, TP79, Tei77, Sig25].

This handle body decomposition is strongly related to *Lê polyhedra* [Lê88, LM17], which inspired our construction of the spine. They cannot, however, be defined over the whole base space of the Milnor fibration, as this would imply periodicity for the monodromy. The spine, in contrast, is well defined for every angle, at the cost of not giving a locally trivial family. As a result, however, this allows us to study the monodromy acting directly on the cells in the spine.

These results are used in two ways. Firstly, they are implemented in computer code, written in Python, and relying on Singular for calculating resolutions, which allows for fast computation of the integral monodromy and variation map. This code is publicly available in a GitHub repository in [PS25a]. Secondly, we introduce the notion of a *gyrograph*, which is an extra structure on a graph that can be understood as a version of tête-à-tête graphs (see [A'C10] for the original definition). This structure recovers completely the algebraic monodromy and variation map, with integral coefficients. Rather than introducing a metric on each edge, this

structure requires angles between adjacent edges at certain vertices of the graph, as well as a filtration, by putting rational weights on each vertex. The invariant spine introduced here is naturally endowed with the structure of a gyrograph, the weights being given essentially by the *Hironaka numbers*, introduced in [TMW01], which are ratios of divisorial valuations of the defining equation of the plane curve, and a generic linear function. This result is materialized in [Theorem 8.2.3](#). Therefore, this approach further underlines the importance of the role of Hironaka numbers in the investigation of the monodromy of a plane curve. The gyrograph construction makes feasible the calculation of the algebraic monodromy and variation map, with integral coefficients, by hand.

Outline of the paper

The paper is structured to go from the purely combinatorial data of the resolution graph to the analytic geometry of the singularity, and finally to the algebraic computation of its invariants. We begin in [Section 2](#) by establishing the requisite combinatorial framework. We define the resolution graph Γ not merely as a topological object, but as a directed graph rooted at the blow-up of the origin. We introduce the notion of a “nice” total ordering on the branches of the curve, which allows us to induce a unique total order on the vertices of the graph. This ordering is crucial for the subsequent consistent labeling of charts and gluing maps.

In [Section 3](#), we translate this combinatorial data into a concrete geometric object. We construct a complex manifold Y by gluing local analytic charts (U_i, \tilde{U}_i) according to the directed edges and labeling functions defined previously. Within this analytic model, we define the function f and a regular sequence of parameters, ensuring that the divisor structure matches the resolution graph. This construction provides the local coordinates necessary for our later dynamical analysis.

The topological realization of the Milnor fibration is developed in [Subsection 3.4](#). We perform the real oriented blow-up of our analytic model to obtain a manifold with corners. A central object of our study, the *invariant A’Campo space* A^{inv} , is constructed here as a union of Seifert-fibered spaces over the real blow-up of the exceptional divisors, connected by interpolating thickened tori. This space serves as the domain for the geometric monodromy and the support for the vector field that drives our homological calculations.

The dynamical core of the paper is in [Subsection 3.5](#) and [Section 5](#). We define a horizontal vector field ξ^{inv} on A^{inv} by lifting gradient fields defined on the exceptional divisors. We provide a detailed local analysis of this vector field, characterizing its singular locus, which consists of non-degenerate saddle points and specific multipronged singularities arising from “dead branches” (bamboos ending at valency 1 vertices) of the resolution graph. This analysis follows closely that of [?]. A key analytic result is established in [Theorem 5.2.2](#), where we prove that the set of “non-generic” angles (those values in the circle $\mathbb{R}/2\pi\mathbb{Z}$ for which saddle connections occur) is finite, thereby ensuring the stability of our topological models for generic angles.

In [Section 6](#), we transition from dynamics to algebra. We construct a 1-dimensional chain complex (C_θ, d_θ) generated by the stable manifolds of the vector field, and a dual complex C_θ^\vee generated by the unstable manifolds. We prove that these are quasi-isomorphic to the absolute and relative singular chain complexes of the Milnor fiber, respectively. This identification allows us to define the algebraic monodromy matrix B_θ (at the level of the chain complexes) explicitly in terms of the intersection numbers of the flow trajectories on the invariant A’Campo space.

Building on this algebraic framework, [Section 7](#) focuses on the variation operator. We define a linear map V at the chain level, acting from the dual complex to the primal complex. We prove that this operator induces the classical variation map on homology, providing a bridge between our Morse-theoretic construction and classical singularity theory.

On [Section 8](#) introduces the theory of “gyrographs” as a computational application of our results. We show that the invariant spine of the fiber, when equipped with weights derived from the Hironaka numbers of the resolution, forms a gyrograph ([Theorem 8.2.3](#)).

Finally, on [Section 9](#) we explain briefly how to use the implemented software [[PS25a](#)] that realizes the computation of algebraic monodromy and variation operator.

2 Preparation

Let $(C, 0) \subset (\mathbb{C}^2, 0)$ be a plane curve defined by a germ $f \in \mathcal{O}_{\mathbb{C}^2, 0}$.

2.1 Initial data

We take as initial data the resolution graph Γ of a plane curve $(C, 0) \subset (\mathbb{C}^2, 0)$ together with a total order of the branches C_1, \dots, C_r .

Let $\pi_0 : (Y_0, D_0) \rightarrow (\mathbb{C}^2, 0)$ be the blow up of \mathbb{C}^2 at the origin. And let \tilde{C} be the strict transform of C in Y_0 . Let t be the number of distinct tangents of $(C, 0)$. In this way, \tilde{C} intersects D_0 in t points $\{p_1, \dots, p_t\}$ and, since Y_0 is smooth, each germ (\tilde{C}, p_ℓ) with $\ell \in \{1, \dots, t\}$ is a plane curve whose branches correspond to a subset of the branches of $(C, 0)$.

Notation 2.1.1. Let $Y \rightarrow \mathbb{C}^2$ be a resolution of the plane curve defined by f . We define the associated dual graph Γ .

Vertices of Γ The set of vertices of Γ , denoted \mathcal{W} , is the disjoint union of two sets: $\mathcal{W} = \mathcal{V} \cup \mathcal{A}$.

- ⌘ The first set is $\mathcal{V} = \{0, 1, \dots, s\}$.
- ⌘ The second set, \mathcal{A} , is in bijection with the set of irreducible branches of the curve $(C, 0)$. We write this curve as the union of its branches: $(C, 0) = \bigcup_{a \in \mathcal{A}} (C_a, 0)$.

Divisors and Edges of Γ Each vertex $w \in \mathcal{W}$ corresponds to a divisor D_w in Y . For the vertices $a \in \mathcal{A}$, the divisor D_a is the strict transform of the corresponding branch C_a in Y .

The edges of Γ are defined by the intersection of these divisors. An edge ij connects two distinct vertices $i, j \in \mathcal{W}$ if and only if their associated divisors intersect: $D_i \cap D_j \neq \emptyset$. In the case of such an intersection, we denote the intersection point as $p_{ij} = D_i \cap D_j$.

We denote by \mathcal{W}_i the set of *neighbor vertices* of the vertex i , that is, the vertices that are adjacent to i .

Associated Divisor Sets We define several collections of divisors.

- ⌘ $D_{\mathcal{V}} = \bigcup_{i \in \mathcal{V}} D_i$, which we also denote as D .
- ⌘ $D_{\mathcal{A}} = \bigcup_{a \in \mathcal{A}} D_a$, the union of all strict transforms.
- ⌘ $D_{\mathcal{W}} = \bigcup_{w \in \mathcal{W}} D_w = D_{\mathcal{V}} \cup D_{\mathcal{A}}$, the total divisor associated with Γ .

For a single divisor D_i (where $i \in \mathcal{W}$), we also define the subset D_i° which consists of the points in D_i that do not lie on any other divisor D_j (for $j \neq i$):

$$D_i^\circ = D_i \setminus \bigcup_{j \in \mathcal{W} \setminus \{i\}} D_j.$$

Graph Properties The graph Γ is a tree, as established in [[Wal04](#), Section 3.6]. A direct consequence of Γ being a tree is that for any two vertices j, k in its vertex set, there exists a unique shortest path connecting them. This unique path is also the *geodesic*, meaning it is the path with the smallest possible number of edges.

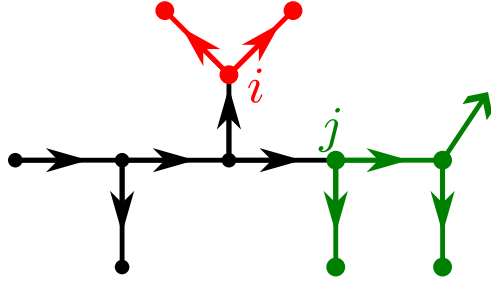


Figure 2.1.1: The resolution graph of a plane curve with its directed structure. In green the branch $\Gamma[j]$ of Γ at j and in red, $\Gamma[i]$.

The dual graph as a directed graph

We endow Γ with the structure of a directed graph and recall (see [PS25b, Section 3]) the definition of the maximal cycle.

Definition 2.1.2. Denote by Z_{\max} the *maximal cycle* in Y , and denote by $c_{0,i}$ its coefficients. Thus,

$$Z_{\max} = \sum_{i \in \mathcal{V}} c_{0,i} D_i.$$

and we have $c_{0,i} = \text{ord}_{D_i}(\ell)$, where $\ell : \mathbb{C}^2 \rightarrow \mathbb{C}$ is a generic linear function. Here *generic* means that the strict transform of $\{\ell = 0\}$ intersects D_0° , or equivalently, that $\{\ell = 0\}$ is not a tangent of C at the origin.

Since $c_{0,i} = \text{ord}_{D_i}(\ell)$ we can similarly define these numbers for arrowheads, that is for $i \in \mathcal{A}$. In this case $c_{0,i} = \text{ord}_{D_i}(\ell) = 0$.

Definition 2.1.3. The graph Γ is seen as a directed graph as follows. Let i, j be neighbors in Γ . The edge ji is directed from j to i if and only if i is further from 0 than j .

A vertex $u \in \mathcal{W}_\Gamma$ is called an *ancestor* of a vertex $v \in \mathcal{W}_\Gamma$ if there exists a directed path from u to v .

We denote by \mathcal{V}_i^+ the neighbors $k \in \mathcal{V}_i$ with $i \rightarrow k$.

Definition 2.1.4. Let i be a vertex in the directed graph Γ , as above. If $i \neq 0$, let j be the unique neighbor of i such that $j \rightarrow i$. The *branch* (fig. 2.1.1) of Γ at i is

- (i) Γ , if $i = 0$ and,
- (ii) otherwise, the connected component of Γ with the edge ji removed, containing i .

The *branch* of Γ at i is denoted by $\Gamma[i]$. We denote by $\mathcal{A}[i]$ the set of arrowheads in $\Gamma[i]$. We say that a branch is *dead* if it contains no arrowheads in it.

Definition 2.1.5. A total order $>$ of the set of branches $\{C_1, \dots, C_r\}$ of a plane curve is said to be *nice* if the following is satisfied

- (i) When $r = 1$ the unique total order is nice
- (ii) If C_a and C_b have the same tangent and it is different from the tangent of C_c , then $C_a > C_c$ if and only if $C_b > C_c$.
- (iii) The total order induced on the plane curves (\tilde{C}, p_ℓ) is nice for all $\ell \in \{1, \dots, t\}$.

Remark 2.1.6. (i) By (ii), a nice total order induces a total order on the set of tangents.

- (ii) Conversely, if we equip each of the plane curves (\tilde{C}, p_ℓ) with a nice total order, then, any total order of the tangents of $(C, 0)$ induces a nice total order on the set of branches of $(C, 0)$.

Lemma 2.1.7. *Any plane curve $(C, 0)$ admits a nice total order.*

Proof. We use induction on the number σ of blow ups needed for the minimal embedded resolution. If $\sigma = 0$, then $(C, 0)$ is smooth and, in particular, it has one single branch and [Definition 2.1.5 \(i\)](#) yields the result.

If $\sigma > 0$, the induction hypothesis applies to the plane curves (\tilde{C}, p_ℓ) , $\ell = 1, \dots, t$. Thus, by [Remark 2.1.6 \(ii\)](#), it suffices to choose a total order of the tangents of $(C, 0)$. ■

Notation 2.1.8. Let $<$ be a nice total order on the set of branches $\{C_1, \dots, C_r\}$ of a plane curve $(C, 0)$. We write $\mathcal{A}[\ell] < \mathcal{A}[k]$ if $C_i < C_j$ for every branch C_i corresponding to an arrowhead in $\mathcal{A}[\ell]$ and every branch C_j corresponding to an arrowhead in $\mathcal{A}[k]$.

Lemma 2.1.9. *Let $(C, 0)$ be a plane curve with a nice total order $<$ on the set of its branches $\{C_1, \dots, C_r\}$. Then there exists a unique total order (that we also denote by $<$) on the set of vertices and arrowheads \mathcal{W}_Γ of the dual graph Γ of the minimal resolution of $(C, 0)$ that satisfies the following two properties.*

- (i) *If $j \rightarrow i$, then $j < i$.*
- (ii) *Assume that $i \rightarrow k$ and $i \rightarrow \ell$ with $k \neq \ell$.*

- ✿ *If $\mathcal{A}[\ell] \neq \emptyset$ and $\mathcal{A}[k] \neq \emptyset$ with $\mathcal{A}[\ell] < \mathcal{A}[k]$, then $u < v$ for every pair of vertices with $u \in \Gamma[\ell]$ and $v \in \Gamma[k]$.*
- ✿ *If $\mathcal{A}[\ell] = \emptyset$ then $u < v$ for every pair of vertices with $u \in \Gamma[\ell]$ and $v \in \Gamma[k]$.*

Proof. We first show the existence by constructing the total order $<$. Let $u, v \in \mathcal{W}_\Gamma$ be two distinct vertices. Since Γ is a directed tree rooted at 0, we have two mutually exclusive cases:

- (i) If u is an ancestor of v (that is, if there is a directed path $u \rightarrow \dots \rightarrow v$), we set $u < v$. Analogously, if v is an ancestor of u , we define $v < u$.
- (ii) If neither u nor v is an ancestor of the other, let $i = \text{LCA}(u, v)$ be their lowest common ancestor. Then there exist distinct children k, ℓ of i such that $i \rightarrow k$, $i \rightarrow \ell$, $u \in \Gamma[k]$, and $v \in \Gamma[\ell]$. Let $\mathcal{A}[k] = \Gamma[k] \cap \mathcal{A}$ and $\mathcal{A}[\ell] = \Gamma[\ell] \cap \mathcal{A}$ be the non-empty sets of branch descendants (identified with the corresponding arrowheads). The given nice total order on \mathcal{A} (denoted $<_{\mathcal{A}}$) is in particular a total order, so it completely orders these sets.
 - ✿ If $\mathcal{A}[k] <_{\mathcal{A}} \mathcal{A}[\ell]$ (that is, if $\forall a \in \mathcal{A}[k], \forall b \in \mathcal{A}[\ell], a <_{\mathcal{A}} b$), we define $u < v$.
 - ✿ If $\mathcal{A}[\ell] <_{\mathcal{A}} \mathcal{A}[k]$, we define $v < u$.

This relation $<$ is total and anti-symmetric by construction. Transitivity follows from a case by case analysis of the LCA's of pairs (u, v) , (v, w) , and (u, w) . This construction satisfies the two properties:

- (i) If $j \rightarrow i$, then j is an ancestor of i , so $j < i$.
- (ii) If $i \rightarrow k$, $i \rightarrow \ell$, and $\mathcal{A}[\ell] <_{\mathcal{A}} \mathcal{A}[k]$, then for any $u \in \Gamma[\ell]$ and $v \in \Gamma[k]$, their LCA is i . And we have already seen that $\mathcal{A}[\ell] <_{\mathcal{A}} \mathcal{A}[k]$ implies $u < v$.

To prove uniqueness, let $<'$ be any total order satisfying properties (i) and (ii). Let $u, v \in \mathcal{W}_\Gamma$ be distinct.

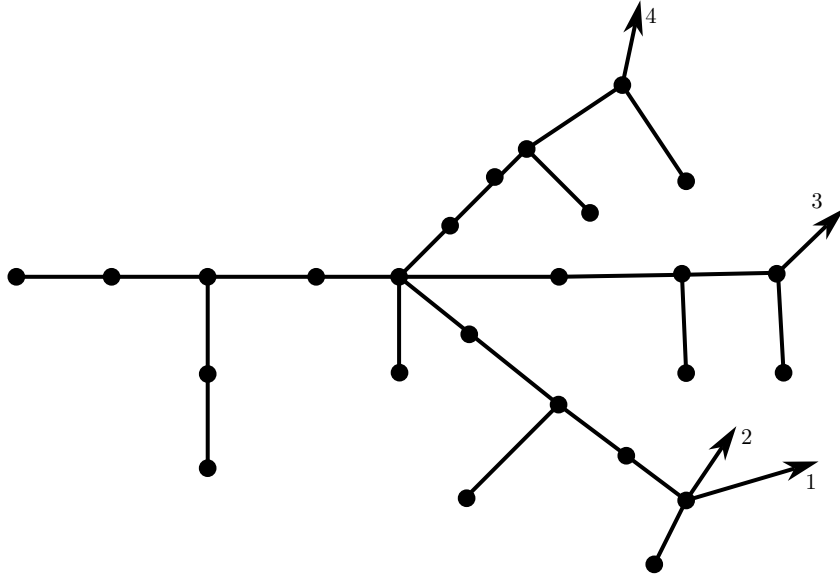


Figure 2.1.2: A nice total order gives a natural embedding of the resolution graph on the real plane \mathbb{R}^2 . The numbers on the arrows indicate the nice total order given on the set of branches as input data for a total order on the set of vertices and arrowheads as defined in [Lemma 2.1.9](#).

- (i) If u is an ancestor of v , there is a path $u = x_0 \rightarrow x_1 \rightarrow \dots \rightarrow x_m = v$. By property (i) for $<'$, $x_j <' x_{j+1}$ for all j . By transitivity of $<'$, $u <' v$. This matches $<$.
- (ii) If u, v are not ancestors, let $i = \text{LCA}(u, v)$ with $u \in \Gamma[k]$ and $v \in \Gamma[\ell]$. Assume $\mathcal{A}[\ell] <_{\mathcal{A}} \mathcal{A}[k]$. Property (ii) states that $u' <' v'$ for every $u' \in \Gamma[\ell]$ and $v' \in \Gamma[k]$. Thus, $v <' u$. This also matches $<$. The case $\mathcal{A}[k] <_{\mathcal{A}} \mathcal{A}[\ell]$ is analogous.

Since $<'$ must agree with $<$ in all cases, the total order is unique. ■

Definition 2.1.10. For each vertex $i \neq 0$ with $j \rightarrow i$. We define a *labeling function* h_i on the set of neighbors of i other than j . We consider two cases and in each of the cases the labeling function preserves the total order of \mathcal{W} .

If i has a nearby dead branch, then

$$h_i : \mathcal{V}_i \setminus \{j\} \rightarrow \{0, \dots, |\mathcal{V}_i^+| - 2\}$$

and, in particular, $h_i(k) = 0$ if k is on the dead branch. Otherwise,

$$h_i : \mathcal{V}_i \setminus \{j\} \rightarrow \{1, \dots, |\mathcal{V}_i^+| - 1\}.$$

A special subgraph

In [PS25b, Section 6] we defined a special subgraph of the dual graph of the minimal embedded resolution. The motivation underlying the definition of this graph was the characterization of the set of divisors to which we could extend (a rescaling of) the vector field $-\nabla \log |f|$. For more on this, we refer the reader to the cited paper. Here we just give a direct definition.

Definition 2.1.11. Let $\Upsilon \subset \Gamma$ be the smallest connected subgraph of Γ containing the vertex corresponding to the first blow-up $0 \in \mathcal{V}$, as well as any vertex in \mathcal{V} adjacent to an arrow-head $a \in \mathcal{A}$. Let $\mathcal{V}_{\Upsilon} \subset \mathcal{V}$ be the vertex set of Υ . We call the vertices of Υ *invariant vertices*.

3 Construction of an analytic model

In the previous section, we established the purely combinatorial data of the singularity, consisting of the dual graph Γ equipped with a directed structure and a total order on its vertices \mathcal{W}_Γ .

We now proceed to construct a geometric object that realizes this combinatorial data. We will build a complex manifold Y by gluing together simple analytic charts (U_i, \tilde{U}_i) . The gluing process itself will be dictated by the directed edges and the labeling function h_i from [Definition 2.1.10](#). This manifold Y will serve as an explicit model for the resolution space of a singularity.

3.1 Analytic charts

For each $i \in \mathcal{V}$, define charts

$$U_i = \mathbb{C} \times D_\delta^2, \quad \tilde{U}_i = \mathbb{C} \times D_\delta^2,$$

where $D_\delta^2 \subset \mathbb{C}$ is a disk of a small radius δ . Let \sim be the equivalence relation on their disjoint union generated by

$$(3.1.1) \quad U_i \ni (u, v) \sim (uv^{b_i}, v^{-1}) \in \tilde{U}_i, \quad u \in D_\delta^2, v \in \mathbb{C}^*,$$

for any $i \in \mathcal{V}$

$$(3.1.2) \quad \tilde{U}_i \ni (u, v) \sim (v, u + h_j(i)) \in U_j, \quad u, v \in D_\delta^2,$$

for any edge $j \rightarrow i$. We then set

$$Y = \coprod_{i \in \mathcal{V}} (U_i \sqcup \tilde{U}_i) / \sim.$$

Then Y is a complex manifold with charts U_i and \tilde{U}_i with coordinates u_i, v_i and \tilde{u}_i, \tilde{v}_i .

Furthermore, we have a compact rational curve $D_i \subset Y$ for each $i \in \mathcal{V}$ defined by $u_i = 0$ in U_i and $\tilde{u}_i = 0$ in \tilde{U}_i . It follows from [eq. \(3.1.1\)](#) that the Euler number of the normal bundle of D_i in Y is $-b_i$. Also, D_i and D_j intersect precisely when ji is an edge in Γ , by [eq. \(3.1.2\)](#). Therefore, the dual graph to this configuration of curves is Γ . As a result, using the Castelnuovo criterion, Y blows down to a smooth surface, which we call Y_{-1} . We get a map

$$\pi : Y \rightarrow Y_{-1}$$

which is a modification of the surface Y_{-1} . Let $o \in Y_{-1}$ be the image of D_V by π .

If $j \rightarrow i$ is a directed edge, then, in the coordinates u_j, v_j , the set $U_j \cap D_i$ is given by $v_j = h_j(i)$. We also have a noncompact curve $D_a \subset Y$ given by $v_i = h_i(a)$ for each $a \in \mathcal{A}$ adjacent to $i \in \mathcal{V}$. Denote by C_a the image of D_a in Y_{-1} under π . Thus C_a is the image of a good parametrisation and therefore, a complex curve in Y_{-1} by [[Wal04](#), Lemma 2.3.1]. Then there exists an

$$f_a \in \mathcal{O}_{Y_{-1}, o}$$

such that the germ (C_a, o) with its reduced analytic structure is the hypersurface germ defined by f_a at $o \in Y_{-1}$, in other words

$$(Z(f_a), o) = (C_a, o).$$

We define $f \in \mathcal{O}_{Y_{-1}, o}$ by

$$(3.1.3) \quad f = \prod_{a \in \mathcal{A}} f_a^{m_a}.$$

3.2 A regular sequence

The sets $\tilde{U}_0 \setminus U_0$ and $U_0 \setminus \tilde{U}_0$ are curvettes to the divisor D_0 . By the same argument as above, there exist functions $x, y \in \mathcal{O}_{Y_{-1}, o}$ such that the germs given by $x = 0$ and $y = 0$ are reduced, and their strict transforms in Y are these curvettes which intersect D_0° transversely. It follows that x, y represents a basis of $\mathfrak{m}_{Y_{-1}, o}/\mathfrak{m}_{Y_{-1}, o}^2$, i.e. x, y is a regular sequence of parameters in $\mathcal{O}_{Y_{-1}, o}$. As a result, we have an isomorphism

$$(3.2.1) \quad \mathcal{O}_{Y_{-1}, o} \simeq \mathbb{C}\{x, y\}.$$

By construction, the coordinate axis $x = 0$ and $y = 0$ are not tangent to the curve $(C, 0)$. Therefore, if $i \in \mathcal{V}$, then $\text{ord}_{D_i}(x) = \text{ord}_{D_i}(y) = c_{0,i}$ (recall [Definition 2.1.2](#)). In particular, the pullback π^*x vanishes with order 1 along D_0 , and the restriction of

$$\frac{\pi^*x|_{U_0}}{u_0}$$

to $\{u_0 = 0\} = U_0 \cap D_0$ is a polynomial in v which vanishes with order $c_{0,\ell}$ at $h_0(\ell)$. Therefore, there exists an $a \in \mathbb{C}^*$ such that

$$\left. \frac{\pi^*x|_{U_0}}{u_0} \right|_{U_0 \cap D_0} = a \prod_{\ell \in \mathcal{V}_0} (v_0 - h_0(\ell))^{c_{0,\ell}}.$$

Similarly, since $\pi^*y|_{U_0}$ also vanishes with order one along $v_0 = 0$ there is a $b \in \mathbb{C}^*$ so that

$$\left. \frac{\pi^*y|_{U_0}}{u_0} \right|_{U_0 \cap D_0} = bv_0 \prod_{\ell \in \mathcal{V}_0} (v_0 - h_0(\ell))^{c_{0,\ell}}.$$

We will assume that x, y are chosen in such a way that $a = b = 1$. In particular,

$$\left. \frac{\pi^*y}{\pi^*x} \right|_{U_0 \cap D_0} = v_0.$$

In fact, since the fraction y/x defines a meromorphic function on Y_{-1} whose only pole is along $\{x = 0\}$, its pullback restricts to a holomorphic function on any D_i for $i \in \mathcal{V} \setminus \{0\}$. As a result, if $i \in \mathcal{V} \setminus \{0\}$, then i is on one of the branches $\Gamma[\ell]$ where ℓ is a neighbor of 0, and

$$\left. \frac{\pi^*y}{\pi^*x} \right|_{D_i} \equiv h_0(\ell).$$

3.3 Local expressions for f

Fix a vertex $i \in \mathcal{V}$ and let $\ell \in \mathcal{V}_i^+$, that is, an adjacent vertex with $i \rightarrow \ell$. By construction π^*f has a zero of order m_ℓ (resp. m_i) along D_ℓ (resp. D_i). Therefore, the function $\pi^*f|_{U_i \cap \tilde{U}_\ell}$ expanded near the point $D_i \cap D_\ell = (0, h_i(\ell))$ on coordinates u_i, v_i , is of the form

$$(3.3.1) \quad \pi^*f(u_i, v_i)|_{U_i \cap \tilde{U}_\ell} = u_i^{m_i} (v_i - h_i(\ell))^{m_\ell} (a_{i\ell} + \text{h.o.t.})$$

where $a_{i\ell} \in \mathbb{C}^*$. In coordinates $\tilde{u}_\ell, \tilde{v}_\ell$, we have a similar expansion

$$\pi^*f(\tilde{u}_\ell, \tilde{v}_\ell)|_{U_i \cap \tilde{U}_\ell} = \tilde{u}_\ell^{m_\ell} \tilde{v}_\ell^{m_i} (a_{\ell i} + \text{h.o.t.}).$$

with $a_{\ell i} \in \mathbb{C}^*$. By [eq. \(3.1.2\)](#), we find

$$a_{i\ell} = a_{\ell i}.$$

Since π^*f has a zero of order m_i along D_i , the fraction $\pi^*f|_{U_i}/u^{m_i}$ defines a holomorphic function in U_i . Its restriction to $U_i \cap D_i = \{u_i = 0\}$ is a polynomial in v_i

$$(3.3.2) \quad \frac{\pi^*(f)|_{U_i}}{u^{m_i}} = a_{ij} \prod_{\ell \in \mathcal{V}_i^+} (v_i - h_i(\ell))^{m_\ell}$$

which has a zero of order m_ℓ at $v_i = h_i(\ell)$ for each $\ell \in \mathcal{V}_i^+$. Let $a_0 \neq 0$ be the leading term of this polynomial, in the case when $i = 0 \in \mathcal{V}$. By replacing f by f/a_0 , we will, from now on, assume that this leading term is 1. As a result, in the case $i = 0$, we have

$$(3.3.3) \quad a_{0k} = \prod_{\substack{\ell \in \mathcal{V}_0 \\ \ell \neq k}} (h_0(k) - h_0(\ell))^{m_\ell}, \quad k \in \mathcal{V}_0.$$

If i is any other vertex in \mathcal{V} other than 0, there exists a $j \in \mathcal{V}$ so that $j \rightarrow i$. By the same argument, we find

$$(3.3.4) \quad a_{ik} = a_{ij} \prod_{\substack{\ell \in \mathcal{V}_i^+ \\ \ell \neq k}} (h_i(k) - h_i(\ell))^{m_\ell}, \quad k \in \mathcal{V}_i^+.$$

Definition 3.3.5. If $i \rightarrow k$ is an edge in Γ , let

$$S_{ik} = \{\ell \in \mathcal{W}_i \mid \ell > k\} = \{\ell \in \mathcal{W}_i \mid h_i(\ell) > h_i(k)\}.$$

See left hand side of [fig. 3.3.1](#).

Definition 3.3.6. Let $i \rightarrow k$ be an edge in Γ , and let $0 = \ell_0 \rightarrow \ell_1 \rightarrow \cdots \rightarrow \ell_{s+1} = k$ be the geodesic connecting 0 and k in Γ . In particular $\ell_s = i$. We define

$$M_{ik} = \sum_{\substack{0 \leq r < s+1 \\ c \in S_{\ell_r \ell_{r+1}}}} m_c.$$

Now let, $0 = \ell_0 \rightarrow \ell_1 \rightarrow \cdots \rightarrow \ell_s = i$ be the geodesic connecting 0 and i , we define

$$M_i = \sum_{k \in \mathcal{V}_i^+} m_k + \sum_{\substack{0 \leq r < s \\ c \in S_{\ell_r \ell_{r+1}}}} m_c.$$

See right hand side of [fig. 3.3.1](#).

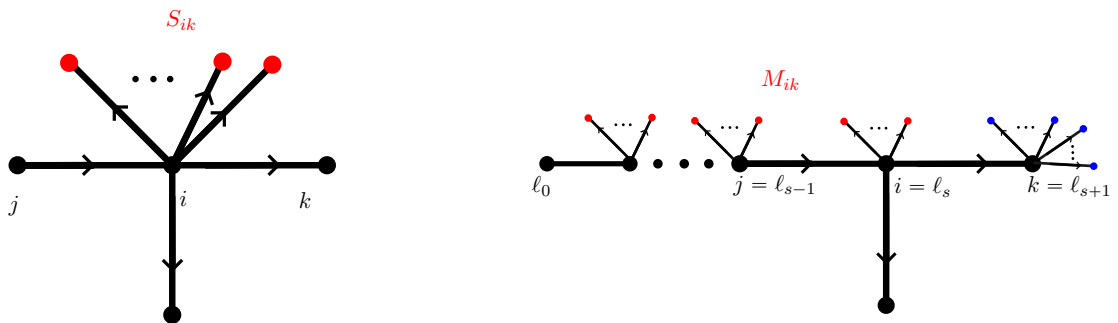


Figure 3.3.1: On the left hand side we see, in red, the vertices that are in S_{ik} . On the right hand side we see: in red the vertices that contribute to M_{ik} ; which together with those in blue are that the vertices that contribute to M_k .

Lemma 3.3.7. Let $i \rightarrow k$ be an oriented edge in Γ . Then, $a_{ik} \in \mathbb{Z} \setminus \{0\}$ and

$$(3.3.8) \quad \text{sign}(a_{ik}) = (-1)^{M_{ik}}$$

Proof. Take signs on both sides of [eq. \(3.3.4\)](#) which gives us

$$\text{sign}(a_{ik}) = \text{sign}(a_{ij})(-1)^{\sum_{h_i(\ell) > h_i(k)} m_\ell}.$$

The result follows from applying the same formula to $\text{sign}(a_{ij})$ and repeating the process iteratively along all the vertices in the geodesic $0 = \ell_0 \rightarrow \ell_1 \rightarrow \dots \rightarrow \ell_{s+1} = k$ connecting 0 and k (with $\ell_s = i$). ■

Lemma 3.3.9. Let $q \in D_{i,\theta}^{\text{ro},\circ}$ be such that its image by Π_i is real. Then, α_i satisfies the following equations depending on where $\Pi_i(q)$ lies:

$$\begin{aligned} m_i \alpha_i(q) &= \theta - M_i \pi && \text{if } -\infty < \Pi_i(q) < 0 \\ m_i \alpha_i(q) &= \theta - M_i \pi && \text{if } -\infty < \Pi_i(q) < 1 && \text{and } i \text{ does not have a neighbor in } \Gamma \setminus \Upsilon \\ m_i \alpha_i(q) &= \theta - M_{ik} \pi && \text{if } h_i(k) < \Pi_i(q) < h_i(k) + 1 && \text{for } k \in \mathcal{V}_i^+ \\ m_i \alpha_i(q) &= \theta - M_{ik} \pi && \text{if } p_i + 1 < \Pi_i(q) < \infty \end{aligned}$$

Proof. By construction, $\arg(q) = \theta$, because $q \in D_{i,\theta}^{\text{ro},\circ}$. By taking argument of both sides of [eq. \(3.3.2\)](#), we get

$$\theta = m_i \alpha_i(q) + \arg \left(a_{ij} \prod_{\ell \in \mathcal{V}_i^+} (v_i - h_i(\ell))^{m_\ell} \right)$$

which, by part [Lemma 3.3.7](#) and [eq. \(3.3.4\)](#), is equivalent to

$$\theta = m_i \alpha_i(q) - \arg((-1)^{M_{ik}}) = m_i \alpha_i(q) - M_{ik} \pi$$

for points q such that $\Pi_i(q)$ lies in between polar points. This proves the third line of the statement. The other 3 lines follow from very similar considerations. ■

3.4 Description of the invariant Milnor fibration

We now use this analytic model to describe the *invariant Milnor fibration*. This involves a topological construction: the real oriented blow-up. In this section we construct a new space, the *invariant A'Campo space* A^{inv} , which is a union of Seifert-fibered pieces over the real-blown-up divisors \hat{D}_i with some interpolating thickened tori. This corresponds to the classical A'Campo space [\[A'C75a\]](#) after contracting some disks to points. The monodromy on these contracted disks is purely periodic.

The real oriented blow-up and the Milnor fibration at radius 0

We start by defining the real oriented blow-up of the resolution space along the exceptional divisors. Here we follow [\[PS25b, Section 4\]](#). Let $(Y, D) \rightarrow (\mathbb{C}^2, 0) \simeq (Y_{-1}, 0)$ be the embedded resolution of our curve singularity. Denote by $\sigma_i : Y_i^{\text{ro}} \rightarrow Y$ the *real oriented blow-up* of Y along the submanifold $D_i \subset Y$ for $i \in \mathcal{W}$ constructed as follows. If $U \subset Y$ is a chart with coordinates u, v such that $u = 0$ is an equation for $D_i \cap U$, then we take a coordinate chart $U^{\text{ro}} \subset Y_i^{\text{ro}}$ with coordinates $r, \alpha, v \in \mathbb{R}_{\geq 0} \times \mathbb{R}/2\pi\mathbb{Z} \times \mathbb{C}$, where r and α are polar coordinates for u , that is:

$$(3.4.1) \quad r = |u| : U^{\text{ro}} \rightarrow \mathbb{R}, \quad \alpha = \arg(u) : U^{\text{ro}} \rightarrow \mathbb{R}/2\pi\mathbb{Z}.$$

We can cover D_i by such charts in order to define an atlas for Y_i^{ro} . In each of these charts, the map σ_i is given by $\sigma_i(r, \theta, v) = (re^{i\theta}, v)$. Denote the fiber product of these maps by

$$(3.4.2) \quad \sigma = \bigtimes_{i \in \mathcal{W}} \sigma_i : (Y^{\text{ro}}, D_{\mathcal{W}}^{\text{ro}}) \rightarrow (Y, D_{\mathcal{W}}).$$

The spaces Y_i^{ro} are manifolds with boundary, and the space Y^{ro} is a manifold with corners and, as a topological manifold, its boundary ∂Y^{ro} coincides with $D_{\mathcal{W}}^{\text{ro}}$.

Notation 3.4.3. The corners of Y^{ro} induce a stratification indexed by the graph Γ as follows. Set $D_{\emptyset}^{\text{ro}} = Y^{\text{ro}} \setminus D_{\mathcal{W}}^{\text{ro}}$. For $i, j \in \mathcal{W}$, we define the following subspaces of ∂Y^{ro} :

$$D_i^{\text{ro}, \circ} = \sigma^{-1}(D_i^\circ), \quad D_i^{\text{ro}} = \sigma^{-1}(D_i), \quad D_{i,j}^{\text{ro}} = \sigma^{-1}(D_i \cap D_j).$$

Note that $\sigma^{-1}(D_i) = \overline{D_i^{\text{ro}, \circ}}$.

The *Milnor fibration at radius zero* is the locally trivial topological fibration given by the map

$$\arg(f^{\text{ro}})|_{\partial Y^{\text{ro}}} : \partial Y^{\text{ro}} \rightarrow \mathbb{R}/2\pi\mathbb{Z}.$$

Definition 3.4.4. For $\theta \in \mathbb{R}/2\pi\mathbb{Z}$, we define the *Milnor ray* at angle θ , as

$$\text{Tub}_\theta^* = \arg(f)^{-1}(\theta) \subset \text{Tub}^*,$$

as well as the subsets of Y^{ro} :

$$(3.4.5) \quad \begin{aligned} Y_\theta^{\text{ro}} &= \arg(f^{\text{ro}})^{-1}(\theta), & D_{i,\theta}^{\text{ro}} &= Y_\theta^{\text{ro}} \cap D_i^{\text{ro}}, \\ D_{i,\theta}^{\text{ro}, \circ} &= Y_\theta^{\text{ro}} \cap D_i^{\text{ro}, \circ}, & D_{i,j,\theta}^{\text{ro}} &= Y_\theta^{\text{ro}} \cap D_{i,j}^{\text{ro}}. \end{aligned}$$

The invariant A'Campo space

Definition 3.4.6. For $i \in \mathcal{V}_\Upsilon$, let

$$\hat{\sigma}_i : \hat{D}_i \rightarrow D_i$$

be the real oriented blow-up of D_i at intersection points $D_i \cap D_\ell$ corresponding to adjacent edges $i \rightarrow \ell$ or $\ell \rightarrow i$ in Υ (see [fig. 3.4.1](#)).

Notation 3.4.7. If i has a neighbor in $\Gamma \setminus \Upsilon$ (equivalently if the minimum of h_i is 0), denote by $q_{i,0} \in \hat{D}_i$ the unique preimage point $\hat{\sigma}_i^{-1}(\{v_i = 0\})$.

3.4.8. In order to construct the invariant A'Campo space, we start by defining a possibly singular Seifert fibration over D_i for each $i \in \mathcal{V}_\Upsilon$. Let

$$A_i^{\text{inv}}$$

be the quotient space of D_i^{ro} obtained by collapsing each connected component of $D_{ik,\theta}^{\text{ro}}$ to a point, for each $\theta \in \mathbb{R}/2\pi\mathbb{Z}$, and for each edge ik in $\Gamma \setminus \Upsilon$. Note that each invariant $i \in \mathcal{V}$ (recall [Definition 2.1.11](#)) can have at most one adjacent edge that is not in Υ . As a result, we have a Seifert fibration

$$\Pi_i : A_i^{\text{inv}} \rightarrow \hat{D}_i$$

which has at most one singular fiber

$$O_i = \Pi_i^{-1}(q_{i,0}).$$

The function $\arg(f)$ induces a horizontal fibration

$$H_i : A_i^{\text{inv}} \rightarrow \mathbb{R}/2\pi\mathbb{Z}.$$

For each $\theta \in \mathbb{R}/2\pi\mathbb{Z}$, denote by $A_{i,\theta}^{\text{inv}} = H_i^{-1}(\theta)$ the fiber. Then, the restriction of Π_i

$$\Pi_{i,\theta} : A_{i,\theta}^{\text{inv}} \rightarrow \hat{D}_i$$

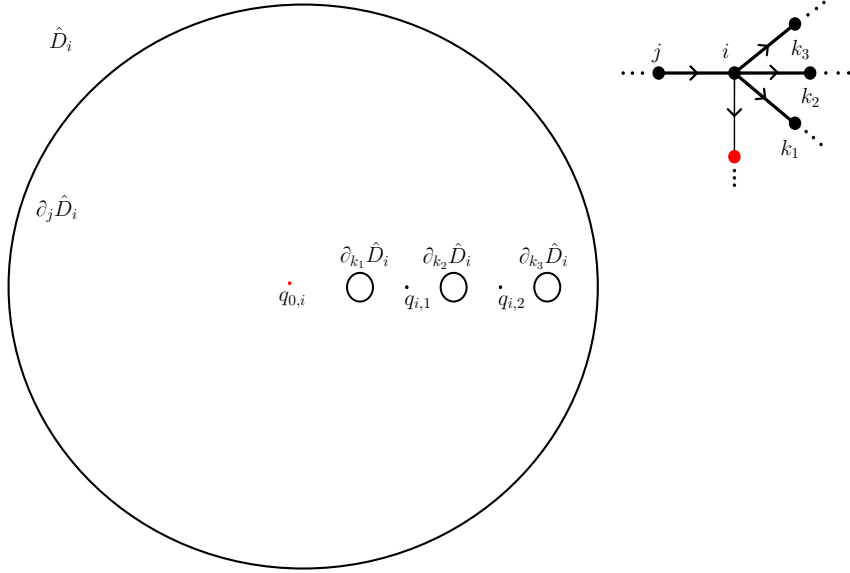


Figure 3.4.1: A representation of \hat{D}_i corresponding to a vertex i with four neighbor invariant vertices j, k_1, k_2 and k_3 (with $j \rightarrow i$); and one vertex in $\Gamma \setminus \Upsilon$ (in red). We can also see the two points of intersection, p_1 and p_2 , of \hat{D}_i with the strict transform of the generic polar curve. In this case $h_i(k_s) = s$ for $s = 1, 2, 3$.

is a branched covering of degree m_i with branching locus $O_{i,\theta} = O_i \cap A_{i,\theta}^{\text{inv}}$. Denote by

$$G_{i,\theta} : A_{i,\theta}^{\text{inv}} \rightarrow A_{i,\theta}^{\text{inv}}$$

the generator of the Galois group of this cover obtained by following Seifert fibers in the direction where H_i increases. Then, A_i^{inv} is the mapping torus (using an interval of length 2π) of $G_{i,\theta}$ for any θ , and H_i is the usual projection to $\mathbb{R}/2\pi\mathbb{Z} = [0, 2\pi]/0 \sim 2\pi$.

For any neighbor k of i in Υ we define $\partial_k A_i^{\text{inv}}$ as the connected component of $\partial A_i^{\text{inv}}$ corresponding to the edge ik . Similarly $\partial_k A_{i,\theta}^{\text{inv}}$ is the part of $\partial A_{i,\theta}^{\text{inv}}$ formed by the collection of $\gcd(m_i, m_k)$ circles that lie in $\partial_k A_i^{\text{inv}}$.

3.4.9. Let $j \rightarrow i$ be an edge in Υ . We use the coordinates (u_j, v_{ji}) on $U_{ji} = U_j \cap \tilde{U}_i$ where $v_{ji} = v_j - h_j(i) = s_{ji}e^{i\beta_{ji}}$ and $u_j = r_j e^{i\alpha_j}$. We use coordinates $(r_j, \alpha_j, s_{ji}, \beta_{ji})$ for

$$U_{ji}^{\text{ro}} = \sigma^{-1}(U_{ji}).$$

In these coordinates, the boundary component $\partial_i A_j^{\text{inv}}$ (corresponding to the edge ij) has coordinates (α_j, β_{ji}) . We also use coordinates $(\tilde{u}_i, \tilde{v}_i)$ on $U_{ji} = U_j \cap \tilde{U}_i$, in this case the induced coordinates on U_{ji}^{ro} are $(\tilde{r}_i, \tilde{\alpha}_i, \tilde{s}_i, \tilde{\beta}_i)$.

Now, define the space

$$A_{ji}^{\text{inv}} = [0, 1] \times \mathbb{R}/2\pi\mathbb{Z} \times \mathbb{R}/2\pi\mathbb{Z}.$$

With coordinates t, α, β . The space A_{ji}^{inv} is the interpolating piece of the A'Campo space between the pieces A_j^{inv} and A_i^{inv} . We also have a horizontal fibration on this piece

$$\begin{aligned} H_{ji} : A_{ji}^{\text{inv}} &\rightarrow \mathbb{R}/2\pi\mathbb{Z} \\ (t, \alpha, \beta) &\mapsto \pi M_{ji} + m_j \alpha + m_i \beta \end{aligned}$$

Recall that by [eq. \(3.3.8\)](#), $M_{ji} \in \mathbb{Z}$. Observe that

$$H_{ji}^{-1}(\theta) = \{(t, \alpha, \beta) \in A_{ji}^{\text{inv}} \mid m_j \alpha + m_i \beta = \theta - \pi M_{ji}\}$$

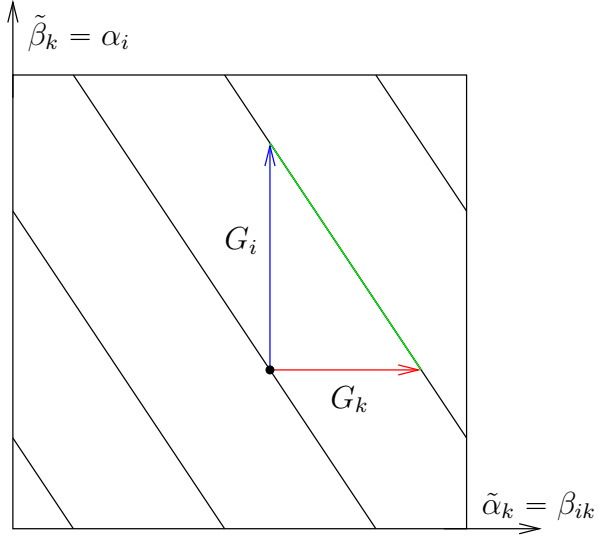


Figure 3.4.2: Suppose that $i \rightarrow k$ is an edge, and that $m_i = 3$ and $m_k = 2$. We see the projection of A_{ik}^{inv} to $(\mathbb{R}/2\pi\mathbb{Z})^2$, with coordinates $(\tilde{\alpha}_k, \tilde{\beta}_k) = (\beta_{ik}, \alpha_i)$. The black subspace is the intersection with a Milnor fiber, given as a level set of $m_i \tilde{\alpha}_i + m_k \tilde{\beta}_k$. The geometric monodromy G_k maps a point with coordinates $(\tilde{\alpha}_k, \tilde{\beta}_k)$ to a point with coordinates $(\tilde{\alpha}_k + 1/3, \tilde{\beta}_k)$, as indicated by the red arrow. Similarly, G_i adds $1/2$ to the α_i coordinate. If we fix some point $x \in (\mathbb{R}/2\pi\mathbb{Z})^2$, we have a segment in $\{x\} \times [0, 1] \subset A_{ik}^{\text{inv}}$. Projecting the image of this segment by $G_{ik} : A_{ik}^{\text{inv}} \rightarrow (\mathbb{R}/2\pi\mathbb{Z})^2$, we get the green segment in the picture, interpolating between G_i and G_k .

is a collection of $m_{ij} = \gcd(m_i, m_j)$ cylinders. We set $A_{ji,\theta}^{\text{inv}} = H_{ji}^{-1}(\theta)$. We define also the map

$$\begin{aligned} G_{ji} : A_{ji}^{\text{inv}} &\rightarrow A_{ji}^{\text{inv}} \\ (t, \alpha, \beta) &\mapsto \left(t, \alpha + 2\pi \frac{1-t}{m_j}, \beta + 2\pi \frac{t}{m_i} \right). \end{aligned}$$

It follows from construction that $G_{ji}|_{A_{ji,\theta}^{\text{inv}}}$ has $A_{ji,\theta}^{\text{inv}}$ as its image and so it defines a map

$$G_{ji,\theta} = G_{ji}|_{A_{ji,\theta}^{\text{inv}}} : A_{ji,\theta}^{\text{inv}} \rightarrow A_{ji,\theta}^{\text{inv}}.$$

We define the gluing maps

$$\begin{aligned} (3.4.10) \quad \partial_i A_j^{\text{inv}} &\rightarrow \{0\} \times (\mathbb{R}/2\pi\mathbb{Z})^2 \subset A_{ji}^{\text{inv}} \\ (\alpha_j, \beta_{ji}) &\mapsto (0, \alpha_j, \beta_{ji}) \end{aligned}$$

and

$$\begin{aligned} (3.4.11) \quad \partial_j A_i^{\text{inv}} &\rightarrow \{1\} \times (\mathbb{R}/2\pi\mathbb{Z})^2 \subset A_{ji}^{\text{inv}} \\ (\tilde{\alpha}_i, \tilde{\beta}_i) &\mapsto (0, \tilde{\beta}_i, \tilde{\alpha}_i) \end{aligned}$$

where $\partial_i A_j^{\text{inv}}$ is the connected component of $\partial A_j^{\text{inv}}$ that corresponds to the edge that connects i with j in Γ .

Definition 3.4.12. We define the *invariant A'Campo space* as the quotient

$$A^{\text{inv}} = \left(\coprod_{i \in \mathcal{V}} A_i^{\text{inv}} \amalg \coprod_{ji \in e(\Gamma)} A_{ji}^{\text{inv}} \right) / \sim$$

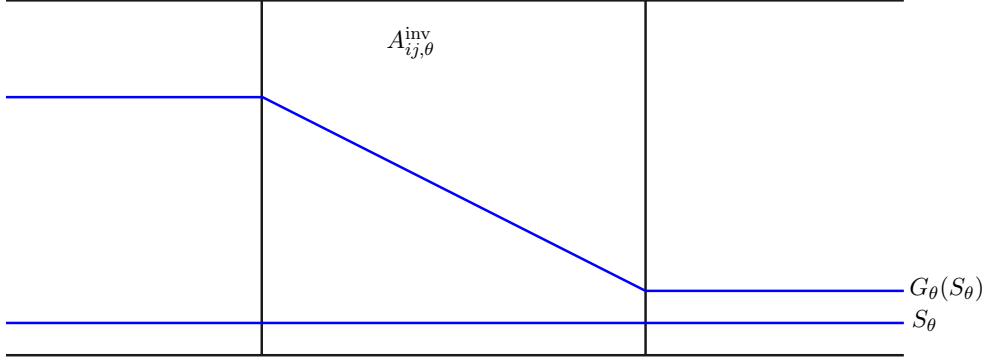


Figure 3.4.3: We see a prong S_θ traversing an interpolating piece $A_{ij,\theta}^{inv}$ and its image $G_\theta(S_\theta)$ by the monodromy.

where \sim is the equivalence relation established by [eqs. \(3.4.10\)](#) and [\(3.4.11\)](#). It follows from construction that the maps H_i and H_{ji} glue together to form a map

$$H : A^{inv} \rightarrow \mathbb{R}/2\pi\mathbb{Z}.$$

We denote $A_\theta^{inv} = H^{-1}(\theta)$. Similarly, the maps G_i and G_{ji} glue together to a map

$$G : A^{inv} \rightarrow A^{inv}.$$

This map leaves A_θ^{inv} invariant for each $\theta \in \mathbb{R}/2\pi\mathbb{Z}$, inducing a monodromy map

$$G_\theta : A_\theta^{inv} \rightarrow A_\theta^{inv}.$$

3.5 Description of the flow

Having constructed the invariant A'Campo space A^{inv} as a fibration $H : A^{inv} \rightarrow \mathbb{R}/2\pi\mathbb{Z}$, we now introduce a dynamical system on this space. We will define a vector field ξ^{inv} that is *horizontal* with respect to this fibration (i.e., tangent to the fibers A_θ^{inv}). The trajectories of this flow will encode the topology of the Milnor fiber. This vector field coincides with the one defined in [\[PS25b\]](#) except over the exceptional divisor D_0 corresponding to the first blow up.

The flow is first defined on the base spaces \hat{D}_i of the Seifert fibrations using a meromorphic function f_i , and then lifted horizontally to the pieces A_i^{inv} . Finally, we will show how these local flows glue together to form a global, well-defined vector field ξ^{inv} on the entire space A^{inv} .

Let $i \in \mathcal{V}$. Then π^*f vanishes with order m_i along D_i , and π^*x vanishes with order $c_{0,i}$ along D_i . As a result, we have a meromorphic function on D_i , defined by

$$(3.5.1) \quad f_i(v_i) = \frac{\pi^*f|_{U_i}^{c_{0,i}}}{\pi^*x|_{U_i}^{m_i}}(0, v_i).$$

This function takes finite nonzero values on D_i° , and has valuation $m_k c_{0,i} - m_i c_{0,k}$ at the intersection point $D_i \cap D_k$, for any $k \in \mathcal{W}$. In fact, if $k \in \mathcal{W}_i^+$, then $m_k c_{0,i} - m_i c_{0,k} = n_{ik} \geq 0$ by [\[PS25b, Lemma 3.4.7\]](#), and if we have a vertex $j \in \mathcal{V}$ such that $j \rightarrow i$, then f_i has a pole of order n_{ij} at $D_i \cap D_j$. Denote by d_i the leading term of this polynomial in the variable v_i . Since π^*f is real by [eq. \(3.3.4\)](#) and π^*x is also real in these coordinates, then $d_i \in \mathbb{R}$. Then

$$(3.5.2) \quad f_i(v_i) = d_i \prod_{\ell \in \mathcal{V}_i^+} (v_i - h_i(\ell))^{n_{i\ell}} = d_i v_i^{n_{ji}} + \text{l.o.t.}$$

where l.o.t. stands for lower order terms in v_i . In the case where $i = 0$, there is no $j \rightarrow 0$ but still we have a similar expression

$$(3.5.3) \quad f_0(v_0) = d_0 \prod_{\ell \in \mathcal{V}_0^+} (v_0 - h_0(\ell))^{n_{i\ell}} = d_0 v_0^{m_0} + \text{l.o.t.}$$

A vector field on \hat{D}_i

Let

$$\xi_i = -\nabla \log |f_i|$$

be the logarithmic gradient vector field of $|f_i|$ defined on D_i° . We claim that by [eq. \(3.5.2\)](#) (see also [fig. 3.4.1](#)), the vector field has exactly one zero $q_{i,a}$ lying on the real segment between the zeroes a and $a+1$ for $1 \leq a \leq \max(h_i - 1) = p_i$ (recall [Definition 2.1.10](#)). Indeed, f'_i has $n_{ij} - 1$ zeroes (one less zero than f_i) counted with multiplicity; it has a zero of order $n_{i\ell} - 1$ at $h_i(\ell)$ for each a and it has at least one zero between each $h_i(\ell)$ on the real line because it is a real polynomial, so the claim follows. We give the same name $q_{i,a}$ to the zeros of pullback vector field on $\hat{D}_i \setminus \partial \hat{D}_i$.

If i has a dead branch attached to it, we denote by $q_{i,0}$ the point that has coordinate $v_i = 0$ in this chart.

If $i = 0$, we denote by $q_{i,-1}$ the point that has coordinate $\tilde{v}_0 = 0$ in $\tilde{U}_0 \cap D_0$.

Notation 3.5.4. We denote by $\Sigma_i \subset D_i$ the union all the $q_{i,a}$ points defined above. Where we recall that $q_{i,0}$ is only there if i has a dead branched attached to it.

We also define the set $\hat{\Sigma}_i = \hat{\sigma}_i^{-1}(\Sigma_i)$.

Remark 3.5.5. The functions v_i and f_i are well defined on $D_i \cap U_i$. From now on, whenever it is convenient we denote by the same symbols the pullback functions $\hat{\sigma}_i^* v_i$ and $\hat{\sigma}_i^* f_i$ defined on \hat{D}_i . We consider the vector field

$$\hat{\sigma}_i^* \xi_i = \hat{\sigma}_i^* (-\nabla \log |f_i|)$$

which is well defined on $\hat{D}_i \setminus \partial \hat{D}_i$. We are going to rescale this vector field now so that it has a non-zero extension to the boundary components of \hat{D}_i . In order to do so, we consider a function

$$\Psi_i : \hat{D}_i \rightarrow \mathbb{R}_+$$

which takes only positive values and,

- (i) in a collar neighborhood of $\partial_k \hat{D}_i$, takes the value $|f_i|^{1/n_{ik}}$ for each neighbor vertex k with $i \rightarrow k$
- (ii) in a collar neighborhood of $\partial_j \hat{D}_i$, it takes the value $|f_i|^{-1/n_{ij}}$ near $\partial_j \hat{D}_i$ where j is the only neighbor with $j \rightarrow i$, if it exists.
- (iii) when $i = 0$ we add the condition that $\Psi_0 = |\tilde{v}_0|^2$ in a neighborhood of $0 \in \tilde{U}_0 \cap D_0$.
- (iv) equals the function $|v_i|^{2(1 - \frac{m_{ik}}{m_i})}$ in a small neighborhood of $q_{i,0} \in \hat{D}_i$ where k is the only adjacent neighbor with $h_i(k) = 0$ in case it exists.

Proposition 3.5.6. *The vector field*

$$\Psi_i \hat{\sigma}_i^* \xi_i$$

extends to all of \hat{D}_i as a vector field $\hat{\xi}_i$, and it points inwards along $\partial_j \hat{D}_i$ when $j \rightarrow i$ and outwards along $\partial_k \hat{D}_i$ for the neighbors k with $i \rightarrow k$. Furthermore,

- (i) *the zero set of $\hat{\xi}_i$ is $\hat{\Sigma}_i$,*
- (ii) *for $1 \leq a \leq p_i$, the singularity $q_{i,a}$ is a non degenerate saddle point of the vector field,*
- (iii) *at $\tilde{v}_0 = 0$ on $\tilde{U}_0 \cap D_0$, the vector field $\hat{\xi}_0$ has a repeller, and*
- (iv) *the trajectories of $\hat{\xi}_i$ are tangent to the level sets of the function $\arg(\hat{\sigma}_i^* f_i)$ or, equivalently, the level sets of $\arg(\hat{\sigma}_i^* f_i)$ are disjoint union of trajectories of $\hat{\xi}_i$.*

Proof. Let k be a neighbor with $i \rightarrow k$. Near the intersection point $D_i \cap D_k$ we consider the coordinate $v_{ik} = v_i - h_i(k)$. By eq. (3.5.2), the function f_i is of the form $v_{ik}^{n_{ik}} g(v_{ik})$ near $D_i \cap D_k$ where $g(v_{ik})$ is a unit. Hence vector field ξ_i is of the form

$$(3.5.7) \quad \xi_i = -\nabla \log |f_i| = -\frac{n_{ik}}{v_{ik}} - \frac{\bar{g}'}{g}$$

So, in polar coordinates (s_{ik}, β_{ik}) with $v_{ik} = s_{ik}e^{i\beta_{ik}}$, the vector field $\hat{\sigma}_i^* \xi_i$ looks like

$$-\begin{pmatrix} n_{ik} s_{ik}^{-1} \\ 0 \end{pmatrix} - \sigma^* \begin{pmatrix} \bar{g}' \\ g \end{pmatrix}.$$

That is, its only non-zero coordinate has a pole of order 1 at $\partial_k \hat{D}_i$. Since the function $|f_i|^{1/n_{ik}}$ extends to and vanishes with order 1 at $\partial_k \hat{D}_i$, we find that $\xi_i = \Psi_i \hat{\sigma}_i^* \xi_i$ extends as a non-zero vector field to $\partial_k \hat{D}_i$. Moreover, since $n_{ik} > 0$, this vector field points outwards.

If $j \rightarrow i$, the argument applies verbatim using the coordinate \tilde{v}_{ij} instead of v_{ik} . The only difference is that f_i has a pole of order n_{ij} instead of a zero and so, in the end, the vector field points inwards. If $i = 0$, we recall the expression eq. (3.5.3) and observe that f_0 has a pole of order m_0 at infinity and so ξ_0 is transverse and points inwards to every sufficiently large circle centered at 0 in the chart U_0 .

By construction, the vector field restricted to $\hat{D}_i \setminus (\partial \hat{D}_i \cup \{q_{i,0}\})$ vanishes on $\sigma_i^{-1}(\Sigma_i)$. That it also vanishes on $q_{i,0}$ follows from Remark 3.5.5, (iv). This proves (i).

Item (ii), follows from the fact that $f'_i(v_i)$ has a simple zero at $q_{i,a}$ and $f_i(q_{i,a}) \neq 0$, so $\overline{\frac{f'_i}{f_i}}$ has a simple saddle point at $q_{i,a}$.

In order to show (iii), we recall eq. (3.5.3) and so eq. (3.5.7) becomes

$$\xi_0 = -\nabla \log |f_0| = \frac{m_0}{\tilde{v}_0} - \frac{\bar{g}'}{g}$$

and so $\hat{\xi}_0$ has the same behavior as the vector field \tilde{v}_0 near $q_{0,-1}$.

The last statement (iv) follows from the expression in eq. (3.5.7) which coincides with $\hat{\xi}_i$ in the interior of \hat{D}_i up to a positive scalar. ■

Definition 3.5.8. We denote by $\hat{\xi}_i$ the extension to all \hat{D}_i of the vector field whose existence is given by the previous lemma.

Let $\ell \in \mathcal{V}_i^+$ be an invariant vertex in Υ and let j be the only vertex with $j \rightarrow i$. Then, by construction, the trajectories of the vector field $\hat{\xi}_i$ that end at $\partial_\ell \hat{D}_i$, start either at $\partial_j \hat{D}_i$ or at a point in $\hat{\Sigma}_i$. Let

$$(3.5.9) \quad \hat{\Delta}_{i\ell} : \partial_\ell \hat{D}_i \dashrightarrow \partial_j \hat{D}_i$$

be the rational map that takes a point $\hat{q} \in \partial_\ell \hat{D}_i$ to the begining in $\partial_j \hat{D}_i$ of the trajectory of $\hat{\xi}_i$ that ends at \hat{q} . Since $\hat{\Sigma}_i$ is finite, this is well defined on an open dense set of $\partial_\ell \hat{D}_i$. The following lemma shows that this map is linear and gives an explicit formula for it.

Lemma 3.5.10. *In the situation above, the map $\hat{\Delta}_{i\ell}$ is a rational linear map defined on $\partial_\ell \hat{D}_i \setminus \{0, \pi\}$ and, when it is defined, it is given by*

$$\hat{\Delta}_{ik}(\hat{q}) = \beta_{ik}(\hat{q}) \frac{n_{ik}}{n_{ij}} + 2\pi \sum_{\ell \in S_{ik}} \frac{n_{i\ell}}{2n_{ij}}$$

if $0 < \arg(v_{ik}(\hat{q})) < \pi$, and

$$\hat{\Delta}_{ik}(\hat{q}) = \beta_{ik}(\hat{q}) \frac{n_{ik}}{n_{ij}} - 2\pi \sum_{\ell \in S_{ik}} \frac{n_{i\ell}}{2n_{ij}}$$

if $-\pi < \arg(v_{ik}(\hat{q})) < 0$.

Proof. The fact that it is rational, is explained in the discussion before the lemma. That it is well defined on $\partial_\ell \hat{D}_i \setminus \{0, \pi\}$ follows from the fact that Σ_i is on the real axis $\{\text{Im}(v_i) = 0\}$ and this real axis is tangent to the flow of ξ_i (see fig. 5.0.1). Because of Proposition 3.5.6 (iv),

$$\arg(\hat{\sigma}_i^* f_i)(\hat{\Delta}_{ik}(\hat{q})) = \arg(\hat{\sigma}_i^* f_i)(\hat{q}).$$

Then, the above formula together with eq. (3.5.2), gives an expression of the form

$$n_{ij} \beta_i(\hat{\Delta}_{ik}(\hat{q})) + a\pi = n_{ik} \beta_{ik}(\hat{q}) + b\pi.$$

where, $a, b \in \{0, 1\}$ depending on the signs of the leading coefficients of f_i . In particular, it gives that the rational function is of the form

$$\hat{\Delta}_{i\ell}(\hat{q}) = \beta_{ik}(\hat{q}) \frac{n_{ik}}{n_{ij}} + \text{independent term}$$

This proves that the rational function is actually linear. Let's find the independent term. Assume, for the moment, that $\ell > k$ for all $k \in \mathcal{V}_i^+$, $k \neq \ell$ and let \hat{q} be such that $\beta_{i\ell}(\hat{q}) = 0$. Since $\hat{\xi}_i$ is tangent to the real axis, we have $\beta_i(\hat{\Delta}_{i\ell}(\hat{q})) = 0$ as well. Substituting in the above formula, gives that the independent term, in this case is 0.

Denote by I_a^+ the points in the circle $\hat{\sigma}_i^{-1}(a)$ where $0 < \beta_{ih_i^{-1}(a)} < \pi$. Equivalently, define I_a^- corresponds with the arc where $\pi < \beta_{ih_i^{-1}(a)} < 2\pi$. By construction, the intervals $\hat{\Delta}_{i\ell}(I_{h_i(k)}^+)$ appear in the order

$$\hat{\Delta}_{i\ell_{p_i+1}}(I_{p_i+1}^+), \hat{\Delta}_{i\ell_{p_i}}(I_{p_i}^+), \dots, \hat{\Delta}_{i\ell_1}(I_1^+), \hat{\Delta}_{i\ell_1}(I_1^-), \dots, \hat{\Delta}_{i\ell_{p_i+1}}(I_{p_i+1}^-)$$

The formula follows, since this gives

$$\lim_{\arg(v_{ik}(q)) \rightarrow 0^\pm} = \pm \pi \sum_{\ell \in S_{ik}} \frac{n_{i\ell}}{n_{ij}}. \quad \blacksquare$$

Lemma 3.5.11. *There exists a smooth vector field ξ_i^{inv} on A_i^{inv} which satisfies*

(i) *it is a lift of the vector field $\hat{\xi}_i$, that is,*

$$D\Pi_i(\xi_i^{\text{inv}}(p)) = \hat{\xi}_i(\Pi_i(p))$$

for all $p \in A_i^{\text{inv}}$

(ii) *It is tangent to the manifolds $A_{i,\theta}^{\text{inv}}$, that is, it is tangent to the horizontal fibration defined by H_i , equivalently*

$$DH_i(\xi_i^{\text{inv}}(p)) = 0$$

for all $p \in A_i^{\text{inv}}$.

Proof. The horizontal fibration defines a connection on the locally trivial fibration

$$\Pi_i|_{A_i^{\text{inv}} \setminus O_i} : A_i^{\text{inv}} \setminus O_i \rightarrow \hat{D}_i \setminus \{q_{i,0}\}$$

so ξ_i^{inv} is determined by items (i) and (ii) on $A_i^{\text{inv}} \setminus O_i$. We define ξ_i^{inv} to be 0 on O_i . In order to finish the proof we need to verify that ξ_i^{inv} is smooth at O_i .

Let k be such that $i \rightarrow k$ and k lies on the only dead branch of i . Near a point in $O_{i,\theta}$ the map $\Pi_{i,\theta}$ is of the form $w \mapsto w^{\frac{m_i}{m_{ik}}}$. We identify tangent vectors to $A_{i,\theta}^{\text{inv}}$ near O_i with complex numbers via the coordinate w . On another hand, near $q_{i,0}$ the vector field $\hat{\xi}_i$ is of the form

$$|v_i|^{2\left(1 - \frac{m_{ik}}{m_i}\right)}$$

So, when pulled back by $\Pi_{i,\theta}$, near a point in $O_{i,\theta}$ takes the form

$$(3.5.12) \quad \left(\frac{m_i}{m_{ik}} w^{\frac{m_i}{m_{ik}} - 1} \right)^{-1} \cdot \left(|v_i|^{2\left(1 - \frac{m_{ik}}{m_i}\right)} \right)_{v_i=w^{\frac{m_i}{m_{ik}}}} = \frac{m_{ik}}{m_i} \bar{w}^{\frac{m_i}{m_{ik}} - 1}.$$

See the left hand side of [fig. 6.1.1](#). ■

The previous lemma defines a vector field ξ_i^{inv} on each piece A_i^{inv} by pulling back the vector field $\hat{\xi}_i$ by the functions $A_{i,\theta}^{\text{inv}} \rightarrow \hat{D}_i$. We denote by $\xi_{i,\theta}^{\text{inv}}$ the restriction $\xi_i^{\text{inv}}|_{A_{i,\theta}^{\text{inv}}}$. We define vector fields ξ_{ji}^{inv} on A_{ji}^{inv} by

$$(3.5.13) \quad \hat{\xi}_{ji} = \begin{pmatrix} 1 \\ 0 \\ 0 \end{pmatrix} = \partial_t$$

Definition 3.5.14. Using [[Mil65](#), Theorem 1.4] together with [Proposition 3.5.6](#) and [eq. \(3.5.13\)](#), we can endow the topological manifold A^{inv} with a C^∞ structure (see also [[PS25b](#), Section 12.3]). This C^∞ structure is the unique one such that the vector fields ξ_i^{inv} and ξ_{ji}^{inv} glue to a smooth a vector field defined on all A^{inv} . We denote this vector field by

$$\xi^{\text{inv}}.$$

Moreover, since this vector field is tangent to A_θ^{inv} , we define

$$\xi_\theta^{\text{inv}} = \xi^{\text{inv}}|_{A_\theta^{\text{inv}}}.$$

We define the sets $\Sigma_i^{\text{inv}} = \Pi^{-1}(\hat{\Sigma}_i)$ and $\Sigma_{i,\theta}^{\text{inv}} = \Pi_\theta^{-1}(\hat{\Sigma}_i)$.

The following lemma follows from the construction of the vector field ξ^{inv} , the definition of the Σ_i sets and [Lemma 3.5.11](#)

Lemma 3.5.15. *The zero set of ξ^{inv} is $\Sigma^{\text{inv}} = \bigcup_{i \in \Upsilon} \Sigma_i^{\text{inv}}$. The zero set of ξ_θ^{inv} is $\Sigma_\theta^{\text{inv}} = \bigcup_{i \in \Upsilon} \Sigma_{i,\theta}^{\text{inv}}$. Furthermore*

- (i) *over each $q_{i,a}$ with $1 \leq a \leq p_i$, the vector field ξ^{inv} has m_i singularities which are saddle points.*
- (ii) *over each $q_{i,0}$ (when it exists) the vector field ξ^{inv} has m_{ik} singularities which are m_i/m_{ik} -pronged singularities. Where $i \rightarrow k$ and k is the only child of i which lies on a dead branch.*

Proof. Item (i) follows from the fact that, over $q_{i,a}$, the vector field ξ^{inv} is a lift via a local diffeomorphism of $\hat{\xi}_i$, and [Proposition 3.5.6\(ii\)](#). Item (ii) follows from [eq. \(3.5.12\)](#). ■

4 The spine

We now define the central object for our combinatorial analysis: the *invariant spine* S_θ^{inv} . This spine is very similar to the one defined in [[PS25b](#), Section 12]: it differs from that one on its definition on the points that lie over $D_{0,\theta}^{\text{ro}}$. This spine is the 1-dimensional CW-complex formed by the union of all stable manifolds of the singularities (critical points) of the flow ξ_θ^{inv} .

Notation 4.0.1. Let $q \in A_\theta^{\text{inv}}$. We denote by

$$\gamma_q : J_q \rightarrow A_\theta^{\text{inv}}$$

the only trajectory of ξ_θ^{inv} that passes through q with $\gamma_q(0) = q$ and $J_q = (J_q^-, J_q^+) \subset \mathbb{R}$ the maximal interval of definition. We define the points $\omega^+(q)$ and $\omega^-(q)$.

$$\omega^\pm(q) = \lim_{t \rightarrow I_q^\pm} \gamma_q(t).$$

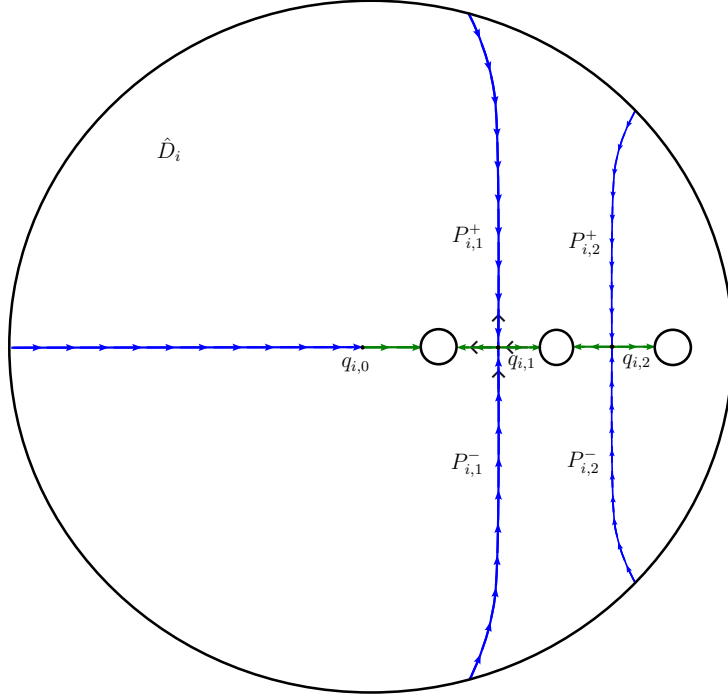


Figure 5.0.1: We see \hat{D}_i with the stable manifolds (in blue) associated with the polar points $q_{i,1}$ and $q_{i,2}$ and the point $q_{i,0}$. In green we see the corresponding unstable manifolds. The black arrows indicate the orientations that prongs take to induce the correct orientation on the chains of $C_{1,\theta}$.

Definition 4.0.2. Let $q \in \Sigma_\theta^{\text{inv}}$ we denote by $S_{q,\theta}^{\text{inv}}$ the union of all the stable manifolds of the singularity q . Since there are no sinks, we find that the set

$$S_\theta^{\text{inv}} = \bigcup_{q \in \Sigma_\theta^{\text{inv}}} \overline{S_{q,\theta}^{\text{inv}}}$$

is a finite 1-dimensional CW-complex. We call it the *relative invariant spine*.

5 Dynamics of the vector field

Recall that by [Proposition 3.5.6 \(ii\)](#) at the points $\{q_{i,a}\}_{1 \leq a \leq p_i}$ the vector field $\hat{\xi}_i$ has saddle points and that $q_{i,a} \in (a, a+1)$. On $D_i^{\text{ro},\circ} \subset A_i^{\text{inv}}$ in the real oriented blow up, we have coordinates (α_i, s_i, β_i) . For each $\theta \in \mathbb{R}/2\pi\mathbb{Z}$, over each $q_{i,a}$ there lie m_i points on $D_{i,\theta}^{\text{ro},\circ} \subset A_{i,\theta}^{\text{inv}}$.

Coordinates of the prongs

Similarly as we did in [eq. \(3.5.9\)](#) we now define a map between boundary components of exceptional divisors in the real oriented blow up.

Definition 5.0.1. Consider an invariant edge $i \rightarrow k$, that is with $i, k \in \mathcal{V}_Y$ and $k \in \mathcal{V}_i^+$. Let $q \in D_{ik}^{\text{ro}}$ with coordinates $(\alpha_i(q), \beta_{ik}(q)) \in (\mathbb{R}/2\pi\mathbb{Z})^2$ and with $\beta_{ik} \notin \{0, \pi\}$. Take the unique trajectory of the vector field ξ_i^{inv} that passes through q . If q lies in $A_{i,\theta}^{\text{inv}}$, then so does this trajectory (because ξ_i^{inv} restricts to a tangent vector field $\xi_{i,\theta}^{\text{inv}}$ on $A_{i,\theta}^{\text{inv}}$). If we follow this trajectory backwards, the next separating torus it passes through is precisely D_{ij}^{ro} with $j \rightarrow i$. Let $\Delta(q)$ be this intersection point. This defines a rational map

$$(5.0.2) \quad \Delta_{ik} : D_{ik}^{\text{ro}} \dashrightarrow D_{ij}^{\text{ro}}$$

that furthermore preserves the angle θ by construction. This map actually lifts the map $\hat{\Delta}_{ik}$ from [eq. \(3.5.9\)](#).

Using the formula from [Lemma 3.5.10](#) we get the following lemma.

Lemma 5.0.3. *Let $q \in D_{ik}^{\text{ro}}$ with $i \rightarrow k$. Then, the trajectory of ξ^{inv} that passes through q , intersects D_{ij}^{ro} with $j \rightarrow i$ in the point $\Delta(q)$ satisfying the following:*

If $0 < \beta_{ik} < \pi$, then

$$\alpha_i(\Delta(q)) = \alpha_i(q) + 2\pi \left(\sum_{\ell \in S_{ik}} \left(\frac{m_\ell}{2m_i} + \left(\frac{m_j}{m_i} - b_i \right) \frac{n_{i\ell}}{2n_{ij}} \right) + \frac{\beta_{ik}(q)}{\pi} \left(\frac{m_k}{2m_i} + \left(\frac{m_j}{m_i} - b_i \right) \frac{n_{ik}}{2n_{ij}} \right) \right)$$

If $\pi < \beta_{ik} < 2\pi$, then

$$\alpha_i(\Delta(q)) = \alpha_i(q) + 2\pi \left(- \sum_{\ell \in S_{ik}} \left(\frac{m_\ell}{2m_i} + \left(\frac{m_j}{m_i} - b_i \right) \frac{n_{i\ell}}{2n_{ij}} \right) + \frac{\beta_{ik}(q) - \pi}{\pi} \left(\frac{m_k}{2m_i} + \left(\frac{m_j}{m_i} - b_i \right) \frac{n_{ik}}{2n_{ij}} \right) \right)$$

If $i = 0$ we have no vertex j with $j \rightarrow i$ but we can define $\alpha_0(\Delta(q))$ by the same formulae, substituting n_{ij} by m_0 .

Proof. Let $q \in D_{ik}^{\text{ro}}$ be a point on the boundary component of A_i^{inv} corresponding to the intersection $D_i \cap D_k$. Let $\Delta(q) \in D_{ij}^{\text{ro}}$ be the point on the boundary component $D_i \cap D_j$ (where $j \rightarrow i$) reached by following the trajectory of ξ^{inv} from q .

The trajectory connecting q and $\Delta(q)$ is a lift of a trajectory $\hat{\gamma}$ of $\hat{\xi}_i$ on \hat{D}_i , which connects $\hat{q} = \Pi_i(q)$ to $\hat{\Delta}(\hat{q}) = \Pi_i(\Delta(q))$. This trajectory $\hat{\gamma}$ must lie on a level set of $\arg(f_i)$, where f_i is the meromorphic function on D_i from [eq. \(3.5.1\)](#). The lifted trajectory γ on A_i^{inv} lies on a fiber of the horizontal fibration H_i , defined by $\theta = \arg(\pi^* f)$.

Let $g_i(v_i) = \pi^* f|_{U_i}/u_i^{m_i}$ be the holomorphic function on $D_i \cap U_i$ defined in [eq. \(3.3.2\)](#):

$$(5.0.4) \quad g_i(v_i) = a_{ij} \prod_{\ell \in \mathcal{V}_i^+} (v_i - h_i(\ell))^{m_\ell}.$$

In the U_i chart we have $u_i = r_i e^{i\alpha_i}$, so the level set is defined by

$$\theta = \arg(\pi^* f) = m_i \alpha_i + \arg(g_i(v_i)).$$

This means that as we flow along the trajectory, the change in the coordinate α_i is determined by the change of $\arg(g_i(v_i))$:

$$m_i \alpha_i(\Delta(q)) - m_i \alpha_i(q) = \arg(g_i(v_i(q))) - \arg(g_i(v_i(\Delta(q)))).$$

The change we want to compute is $\alpha_i(\Delta(q)) - \alpha_i(q)$. From the coordinate change of [eq. \(3.1.1\)](#), we have $\tilde{u}_i = u_i v_i^{b_i}$, which implies $\tilde{\alpha}_i = \alpha_i + b_i \beta_i$, where $\beta_i = \arg(v_i)$. The change in α_i (in the coordinates of the U_i chart) from q to $\Delta(q)$ is

$$(5.0.5) \quad \alpha_i(\Delta(q)) - \alpha_i(q) = \frac{1}{m_i} \left(\arg(g_i(\hat{q})) - \arg(g_i(\hat{\Delta}(\hat{q}))) \right).$$

Let $\beta_{ik}(\hat{q}) = \arg(v_i - h_i(k))$ and $\beta_i(\hat{\Delta}(\hat{q})) = \arg(v_i)$.

We treat the rest of the proof by cases:

Case 1: q is in the “upper half” ($0 < \beta_{ik}(\hat{q}) < \pi$).

⌘ At \hat{q} : as $v_i \rightarrow h_i(k)$ along the trajectory converging to \hat{q} , eq. (5.0.4) gives

$$\arg(g_i(v_i)) \rightarrow \arg(a_{ij}) + m_k \beta_{ik}(\hat{q}) + \pi \sum_{\ell \in S_{ik}} m_\ell \pmod{2\pi}.$$

⌘ At $\hat{\Delta}(\hat{q})$, that is, $v \rightarrow \infty$ along the same trajectory, the constants $h_i(\ell)$ are negligible and we find

$$g_i(v_i) \approx a_{ij} v_i^{\sum m_\ell} = a_{ij} v_i^{m_i b_i - m_j},$$

where the sum in the exponent runs through $\ell \in \mathcal{V}_i^+$, and we use the relation

$$-b_i m_i + \sum_{\ell \in \mathcal{V}_i} m_i = 0, \quad \mathcal{V}_i = \mathcal{V}_i^+ \sqcup \{j\}.$$

As a result,

$$\arg(g_i(v_i)) \rightarrow \arg(a_{ij}) + (m_i b_i - m_j) \beta_i(\hat{\Delta}(\hat{q})) \pmod{2\pi}.$$

Substituting these into the formula for $\alpha_i(\Delta(q)) - \alpha_i(q)$, we find:

$$\begin{aligned} \alpha_i(\Delta(q)) - \alpha_i(q) &= \frac{1}{m_i} \left(m_k \beta_{ik}(q) + \pi \sum_{\ell \in S_{ik}} m_\ell - (m_i b_i - m_j) \beta_i(\Delta(q)) \right) \\ &= \frac{m_k \beta_{ik}(q)}{m_i} + \frac{\pi \sum_{\ell \in S_{ik}} m_\ell}{m_i} + \left(\frac{m_j}{m_i} - b_i \right) \beta_i(\Delta(q)) \end{aligned}$$

From Lemma 3.5.10, we have

$$\beta_i(\Delta(q)) = \frac{n_{ik}}{n_{ij}} \beta_{ik}(q) + \frac{\pi}{n_{ij}} \sum_{\ell \in S_{ik}} n_{i\ell}.$$

Substituting this expression for β_i in the expression obtained before (with $\beta_{ik} = \beta_{ik}(\Delta(q))$):

$$\begin{aligned} \alpha_i(\Delta(q)) - \alpha_i(q) &= \frac{m_k \beta_{ik}}{m_i} + \frac{\pi \sum_{\ell \in S_{ik}} m_\ell}{m_i} + \left(\frac{m_j}{m_i} - b_i \right) \left(\frac{n_{ik}}{n_{ij}} \beta_{ik} + \frac{\pi}{n_{ij}} \sum_{\ell \in S_{ik}} n_{i\ell} \right) \\ &= \beta_{ik} \left(\frac{m_k}{m_i} + \left(\frac{m_j}{m_i} - b_i \right) \frac{n_{ik}}{n_{ij}} \right) + \pi \left(\frac{\sum_{\ell \in S_{ik}} m_\ell}{m_i} + \left(\frac{m_j}{m_i} - b_i \right) \frac{\sum_{\ell \in S_{ik}} n_{i\ell}}{n_{ij}} \right) \end{aligned}$$

Rewriting this by factoring out 2π :

$$= 2\pi \left[\sum_{\ell \in S_{ik}} \left(\frac{m_\ell}{2m_i} + \left(\frac{m_j}{m_i} - b_i \right) \frac{n_{i\ell}}{2n_{ij}} \right) + \frac{\beta_{ik}}{\pi} \left(\frac{m_k}{2m_i} + \left(\frac{m_j}{m_i} - b_i \right) \frac{n_{ik}}{2n_{ij}} \right) \right]$$

This matches the first formula in the lemma.

Case 2: q is in the “lower half” ($\pi < \beta_{ik}(\hat{q}) < 2\pi$). This case follows similarly, using the case $-\pi < \arg(v_{ik}) < 0$ in Lemma 3.5.10.

The case $i = 0$ follows by setting $j = -1$ (the virtual *ancestor vertex* corresponding to \mathbb{C}^2), $m_j = m_{-1} = 0$, and noting that the pole order $n_{ij} = n_{0,-1}$ of f_0 at ∞ is m_0 . ■

5.1 Generic angles

Definition 5.1.1. We say that $\theta \in \mathbb{R}/2\pi\mathbb{Z}$ is a *generic angle* for f if there is no trajectory in A_θ^{inv} connecting two singularities of ξ_θ^{inv} whose stable set has dimension one. Otherwise, we say that θ is *nongeneric*.

We denote the set of non-generic angles by $\Theta_{\text{ng}} \subset \mathbb{R}/2\pi\mathbb{Z}$.

5.2 The set of non-generic angles

In this section, we prove that the set of angles θ for which the topology of the Milnor fiber varies is finite. The following number is a classical invariant and its name is due to [TMW01].

Definition 5.2.1. For any vertex i of the resolution graph Γ , its associated *Hironaka number* is

$$h_i = \frac{m_i}{c_{0,i}}.$$

If a is an arrowhead vertex in Γ , then we set $h_a = +\infty$, and $h_a^{-1} = 0$.

Theorem 5.2.2. *The set of non-generic angles $\Theta_{\text{ng}} \subset \mathbb{R}/2\pi\mathbb{Z}$ is finite.*

Proof. By Definition 5.1.1, an angle θ is non-generic if and only if there exists a trajectory γ of the vector field ξ_θ^{inv} inside the fiber A_θ^{inv} connecting two singularities $p, q \in \Sigma_\theta^{\text{inv}}$ such that:

- (i) $\lim_{t \rightarrow +\infty} \gamma(t) = q$, where q is a singularity with $\dim(W^s(q)) = 1$ (a saddle or a multipronged saddle point).
- (ii) $\lim_{t \rightarrow -\infty} \gamma(t) = p$, where p is a singularity with $\dim(W^u(p)) = 1$ (a saddle or a multipronged saddle point).

Since $\Sigma_\theta^{\text{inv}}$ is a finite set, it suffices to prove that for any fixed pair of vertices $u, v \in \mathcal{V}$ (not necessarily distinct) and any pair of specific separatrices associated with singularities in A_u^{inv} and A_v^{inv} , the set of angles θ allowing a connection is finite.

Recall from eq. (3.5.1) that on each divisor D_i , the geometry of the vector field $\hat{\xi}_i$ is determined by the meromorphic function:

$$f_i = \frac{(\pi^* f)^{c_{0,i}}}{(\pi^* x)^{m_i}}.$$

By Proposition 3.5.6 (iv), the trajectories of $\hat{\xi}_i$ are contained in the level sets of $\arg(f_i)$. Since ξ_θ^{inv} is a lift of $\hat{\xi}_i$ (via the local diffeomorphism $\Pi_{i,\theta}$ away from singular fibers), the function $\arg(f_i)$ is constant along any trajectory γ lying within the piece $A_{i,\theta}^{\text{inv}}$.

The fiber A_θ^{inv} is globally defined by the condition $\arg(\pi^* f) = \theta$. We substitute this into the expression for the argument of f_i :

$$\arg(f_i) \equiv c_{0,i} \arg(\pi^* f) - m_i \arg(\pi^* x) \equiv c_{0,i} \theta - m_i \arg(\pi^* x) \pmod{2\pi}.$$

We can express $\arg(\pi^* x)$ in terms of θ and a local invariants of each vertex. Let $h_i = m_i/c_{0,i}$ be the Hironaka number of the divisor D_i (see Definition 5.2.1). We have:

$$(5.2.3) \quad \arg(\pi^* x) \equiv \frac{c_{0,i}}{m_i} \theta - \frac{1}{m_i} \arg(f_i) \equiv \frac{1}{h_i} \theta - \frac{1}{m_i} \arg(f_i) \pmod{2\pi}.$$

Let γ be a trajectory connecting $p \in A_{u,\theta}^{\text{inv}}$ to $q \in A_{v,\theta}^{\text{inv}}$.

⌘ Near q , the trajectory coincides with a specific stable separatrix of q . Let $K_q \in [0, 2\pi)$ be the constant value of $\arg(f_v)$ along this separatrix. This constant K_q is the argument of f_v evaluated at the saddle point or multipronged point. Thus, along the stable part of γ :

$$\arg(\pi^* x) \equiv \frac{1}{h_v} \theta - \frac{K_q}{m_v} \pmod{2\pi}.$$

⌘ Near p , the trajectory coincides with an unstable separatrix of p . Let $K_p \in [0, 2\pi)$ be the constant value of $\arg(f_u)$ along this separatrix. Similarly, along the unstable part of γ :

$$\arg(\pi^* x) \equiv \frac{1}{h_u} \theta - \frac{K_p}{m_u} \pmod{2\pi}.$$

Since $\arg(\pi^*x)$ is a global function on the ambient space (and the chart gluing maps respect this coordinate), for the unstable manifold of p to connect to the stable manifold of q , their values of $\arg(\pi^*x)$ must coincide. This yields the linear equation:

$$\frac{1}{h_v}\theta - \frac{K_q}{m_v} \equiv \frac{1}{h_u}\theta - \frac{K_p}{m_u} \pmod{2\pi}.$$

Rearranging terms:

$$(5.2.4) \quad \theta \left(\frac{1}{h_v} - \frac{1}{h_u} \right) \equiv \frac{K_q}{m_v} - \frac{K_p}{m_u} \pmod{2\pi}.$$

We claim that if $u \neq v$ are distinct vertices involved in a saddle connection, the coefficient $\Lambda_{uv} = \frac{1}{h_v} - \frac{1}{h_u}$ is generically non-zero. Using the definition of Hironaka numbers:

$$\Lambda_{uv} = \frac{c_{0,v}}{m_v} - \frac{c_{0,u}}{m_u} = \frac{m_u c_{0,v} - m_v c_{0,u}}{m_u m_v}.$$

In the resolution graph of a plane curve singularity, the quantity $n_{uv} = m_u c_{0,v} - m_v c_{0,u}$ is non-zero for any pair of vertices connected by a path in the tree (this relates to the strict monotonicity of the function m/c_0 along geodesics from the root). If $u = v$, then the equation becomes $0 \equiv K_q/m_v - K_p/m_v \pmod{2\pi}$. In this case we just verify that our model does not yield any saddle connections.

Since $\Lambda_{uv} \neq 0$, eq. (5.2.4) has a finite number of solutions for θ in $[0, 2\pi]$. As the number of pairs of singular points and separatrices is finite, the total set Θ_{ng} is finite. ■

6 Algebraic monodromy and variation

In this section, we construct a finite-dimensional chain complex (C_θ, d_θ) that computes the homology of the Milnor fiber. The relative invariant spine has a natural structure of CW-complex and the chain complex that we define in this section is a sub-complex of that one which carries the same homological information but yields computational advantages. The generators of the first level of this complex $C_{1,\theta}$ will be unions of pairs of trajectories converging to the singularities of ξ_θ^{inv} . The generators of $C_{0,\theta}$ are the repellers of the vector field in $A_{0,\theta}^{\text{inv}}$. We will also define a dual complex C_θ^\vee generated by the unstable manifolds.

We will show that these complexes are quasi-isomorphic to the singular chain complexes of A_θ^{inv} (absolute and relative, respectively). This construction provides a concrete algebraic framework on which the monodromy and variation operators can be represented as matrices.

6.1 A chain complex

Fix a vertex $i \in \mathcal{V}_Y$ and a non-generic angle θ .

Chains for saddle points

Choose a saddle point $q_{i,a} \in \hat{D}_i$. Let $q_{i,a,\theta}[1]$ be the point in $\Pi_{i,\theta}^{-1}(q_{i,a})$ whose α coordinate in $[0, 2\pi]$ is closest to 0. Let

$$q_{i,a,\theta}[2], \dots, q_{i,a,\theta}[m_i]$$

be the other $m_i - 1$ points labeled according to the orientation of $\Pi_i^{-1}(q_{i,a})$. Equivalently, the points are labeled so that

$$\alpha_i(q_{i,a,\theta}[b]) \in \left[\frac{2\pi(b-1)}{m_i}, \frac{2\pi b}{m_i} \right] + 2\pi\mathbb{Z} \quad \text{for all } a \in \{1, \dots, p_i\} \text{ and all } b \in \{1, \dots, m_i\}.$$

By Lemma 3.5.15, the vector field ξ^{inv} has saddle points at $q_{i,a,\theta}[b]$. We denote by

$$S_{i,a,\theta}[b] = \overline{(\omega^+)^{-1}(q_{i,a,\theta}[b])}$$

the closure of the stable manifold of ξ^{inv} at $q_{i,a,\theta}[b]$. This stable manifold is naturally partitioned into three sets

$$S_{i,a,\theta}[b] = P_{i,a,\theta}^+[b] \cup \{q_{i,a,\theta}[b]\} \cup P_{i,a,\theta}^-[b]$$

where $P_{i,a,\theta}^+[b]$ is the preimage by $\Pi_{i,\theta}$ of the stable manifold $P_{i,a}^+$ of $\hat{\xi}_i$ at $q_{i,a}$ that lies on the upper half plane; and $P_{i,a,\theta}^-[b]$ the preimage of the stable manifold $P_{i,a}^-$ that lies on the lower half plane (See fig. 5.0.1). We orient $S_{i,a,\theta}[b]$ so that $P_{i,a,\theta}^-[b]$ keeps its orientation induced by the flow of the vector field and $P_{i,a,\theta}^+[b]$ inverts it. See fig. 5.0.1 for a drawing representing these orientations. Similarly, we denote by

$$U_{i,a,\theta}[b] = \overline{(\omega^-)^{-1}(q_{i,a,\theta}[b])}$$

the unstable manifold of ξ^{inv} at that same point. We orient $U_{i,a,\theta}[b]$ in such a way that near the point $q_{i,a,\theta}[b]$, the restriction of $\Pi_{i,\theta}$ to the preimage of the real axis in \hat{D}_i reverses orientation. Similarly as we have done for the stable manifolds, we observe that the unstable manifold is partitioned as

$$U_{i,a,\theta}[b] = R_{i,a,\theta}^+[b] \cup \{q_{i,a,\theta}[b]\} \cup R_{i,a,\theta}^-[b]$$

where $R_{i,a,\theta}^+[b]$ is the preimage by $\Pi_{i,\theta}$ of the stable manifold $R_{i,a}^+$ of $\hat{\xi}_i$ at $q_{i,a}$ that lies to the right of $q_{i,a}$ on the real axis and $R_{i,a,\theta}^-[b]$ is the other one.

If each prong (stable or unstable) is oriented by the flow of $\hat{\xi}_i$, we orient the stable and unstable manifolds like

$$\begin{aligned} S_{i,a,\theta}[b] &= P_{i,a,\theta}^-[b] - P_{i,a,\theta}^+[b] \\ U_{i,a,\theta}[b] &= R_{i,a,\theta}^-[b] - R_{i,a,\theta}^+[b] \end{aligned}$$

These orientations are chosen so that the signed intersection $\langle S_{i,a,\theta}[b], U_{i,a,\theta}[b] \rangle = +1$ is positive.

Chains for multipronged singularities

Next, assume that i has a neighbor $k \in \mathcal{V} \setminus \mathcal{V}_\Gamma$. Note that there can be at most one such k . We label the m_{ik} preimages of $q_{i,0}$ on A_θ^{inv} , by

$$q_{i,0,\theta}[c], \quad \text{with } c \in \mathbb{Z}/m_{ik}\mathbb{Z}.$$

At these points, the vector field ξ^{inv} has m_i/m_{ik} -pronged singularities where each of the prongs lies in a trajectory of ξ^{inv} converging to some $q_{i,0,\theta}[c]$. We label these prongs in a similar way as we labeled the points $q_{i,a,\theta}[b]$. More concretely, let $q_{i,0}^- \in \mathbb{R}_-$ be a point in \hat{D}_i very close to $q_{i,0}$. Using the same criterion as above, we obtain points

$$q_{i,0,\theta}^-[1], \dots, q_{i,0,\theta}^-[m_i]$$

each lying in a different prong. Let

$$P_{i,0,\theta}[b]$$

be the prong where the point $q_{i,0,\theta}^-[b]$ lies. Observe that $P_{i,0,\theta}[b]$ is a prong of the singularity $q_{i,0,\theta}[b \bmod m_{ik}]$. Finally we define the chains

$$(6.1.1) \quad S_{i,0,\theta}[b] = P_{i,0,\theta}[b] \cup P_{i,0,\theta}[b'] \cup \{q_{i,0,\theta}[b \bmod m_{ik}]\}, \quad 1 \leq b \leq m_i - m_{ik}$$

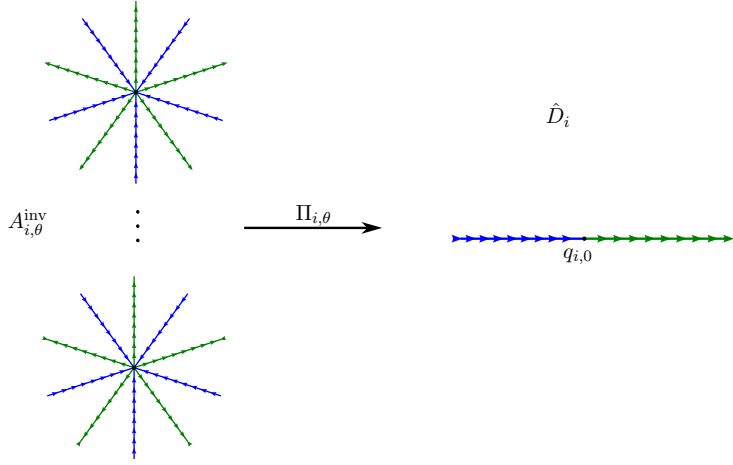


Figure 6.1.1: On the left we see the preimage on $A_{i,\theta}^{\text{inv}}$ of a neighborhood of the point $q_{i,0} \in \hat{D}_i$ by $\Pi_{i,\theta}$.

where b' is the largest element of $\{1, 2, \dots, m_i\}$ which is congruent to b modulo m_{ik} . The prongs $P_{i,0,\theta}[b]$ are oriented, since they are trajectories. We orient the cycle eq. (6.1.1) in such a way that $P_{i,0,\theta}[b]$ has this orientation, and $P_{i,0,\theta}[b']$ has the opposite orientation.

For each b , with $1 \leq b \leq m_i - m_{ik}$, we also define a *dual cycle* to $S_{i,0,\theta}[b]$ as follows. Let R and R' be the two outgoing prongs adjacent to the incoming prong $P_{i,0,\theta}[b]$, as in fig. 6.1.1. Here, R is on the right of $P_{i,0,\theta}[b]$, and R' is on the left. Orient R as incoming, and R' as outgoing. We then set

$$U_{i,0,\theta}[b] = R \cup R' \cup \{q_{i,0,\theta}[b \bmod m_{ik}]\}$$

As in the saddle point case, these orientations are chosen so that the signed intersection $\langle S_{i,0,\theta}[b], U_{i,0,\theta}[b] \rangle = +1$ is positive.

Let $q_{0,-1} \in \hat{D}_0$ be the unique repeller of $\hat{\xi}_0$ as in Proposition 3.5.6, (iii). For any $\theta \in \mathbb{R}/2\pi\mathbb{Z}$, the point $q_{0,-1}$ has precisely $e = m_0$ preimages in $A_{0,\theta}^{\text{inv}}$. Call them $q_{0,-1,\theta}[1], \dots, q_{0,-1,\theta}[e]$, in such a way that for $b = 1, \dots, e$, we have

$$\tilde{\alpha}(q_{0,-1,\theta}[b]) \in \left[\frac{(b-1)2\pi}{e}, \frac{b2\pi}{e} \right).$$

For $1 \leq b \leq e$, we set

$$\begin{aligned} S_{0,0,\theta}[b] &= \{q_{0,-1,\theta}[b]\} = (\omega^+)^{-1}(q_{0,-1,\theta}[b]), \\ U_{0,0,\theta}[b] &= (\omega^-)^{-1}(q_{0,-1,\theta}[b]). \end{aligned}$$

Note that $S_{0,0,\theta}[b]$ is just a point and $U_{0,0,\theta}[b]$ is a topological disk since $q_{0,-1,\theta}[b]$ is a fountain of ξ_θ^{inv} .

Definition 6.1.2. Let $i \in \mathcal{V}_Y$. If $1 \leq a \leq p_i$, set

$$\begin{aligned} C_{1,i,a,\theta} &= \mathbb{Z}\langle S_{i,a,\theta}[b] \mid 1 \leq b \leq m_i \rangle, \\ C_{1,i,a,\theta}^\vee &= \mathbb{Z}\langle U_{i,a,\theta}[b] \mid 1 \leq b \leq m_i \rangle, \end{aligned}$$

as well as

$$\begin{aligned} C_{1,i,0,\theta} &= \mathbb{Z}\langle S_{i,0,\theta}[b] \mid 1 \leq b \leq m_i - m_{ik} \rangle \\ C_{1,i,0,\theta} &= \mathbb{Z}\langle U_{i,0,\theta}[b] \mid 1 \leq b \leq m_i - m_{ik} \rangle \end{aligned}$$

in case i has a neighbor $k \in \mathcal{V}_\Gamma \setminus \mathcal{V}_Y$, otherwise we define $C_{1,i,0,\theta}$ and $C_{1,i,0,\theta}^\vee$ to be trivial \mathbb{Z} -modules. We define

$$\begin{aligned} C_{1,i,\theta} &= \bigoplus_{a=0}^{p_i} C_{1,i,a,\theta}, & C_{1,\theta} &= \bigoplus_{i \in \mathcal{V}_Y} C_{1,i,\theta} \\ C_{1,i,\theta}^\vee &= \bigoplus_{a=0}^{p_i} C_{1,i,a,\theta}^\vee, & C_{1,\theta}^\vee &= \bigoplus_{i \in \mathcal{V}_Y} C_{1,i,\theta}^\vee. \end{aligned}$$

6.1.3. Let

$$I_1 \subset \mathcal{V}_Y \times \mathbb{Z} \times \mathbb{Z}$$

be defined by $(i, a, b) \in I_1$ if and only if $S_{1,i,a,\theta}[b] \in C_{1,\theta}$. By Lemma 2.1.7, the set \mathcal{V}_Y is totally ordered so the set $\mathcal{V}_Y \times \mathbb{Z}_{\leq 0} \times \mathbb{Z}_{\leq 1}$ has a lexicographic order which induces a lexicographic order on I_1 . Similarly, we define

$$I_{1,i} = \{i\} \times \mathbb{Z} \times \mathbb{Z} \cap I_1 \subset I_1$$

and

$$I_{1,i,a} = \{i\} \times \{a\} \times \mathbb{Z} \cap I_{1,i} \subset I_{1,i}$$

We define also

$$\begin{aligned} C_{0,\theta} &= \mathbb{Z} \langle S_{0,0,\theta}[1], \dots, S_{0,0,\theta}[e] \rangle \\ C_{2,\theta}^\vee &= \mathbb{Z} \langle U_{0,0,\theta}[1], \dots, U_{0,0,\theta}[e] \rangle. \end{aligned}$$

Finally, if $j \neq 0, 1$, then let $C_{j,\theta}$ be the trivial \mathbb{Z} -module. Similarly, if $j \neq 1, 2$, then let $C_{j,\theta}^\vee$ be the trivial \mathbb{Z} -module. We then have graded \mathbb{Z} -modules

$$C_\theta = \bigoplus_{j \in \mathbb{Z}} C_{j,\theta}, \quad C_\theta^\vee = \bigoplus_{j \in \mathbb{Z}} C_{j,\theta}^\vee.$$

These graded modules are naturally seen as submodules of the singular chain complex of A_θ^{inv} , and the singular chain complex of A_θ^{inv} relative to $\partial A_\theta^{\text{inv}}$, respectively, that is

$$(6.1.4) \quad C_\theta \subset C(A_\theta^{\text{inv}}; \mathbb{Z}), \quad C_\theta^\vee \subset C(A_\theta^{\text{inv}}, \partial A_\theta^{\text{inv}}; \mathbb{Z}).$$

These are, in fact, subcomplexes, that is, they are invariant under the differential. Denote the restrictions by

$$d_{j,\theta} : C_{j,\theta} \rightarrow C_{j-1,\theta}, \quad d_{j,\theta}^\vee : C_{j,\theta}^\vee \rightarrow C_{j-1,\theta}^\vee.$$

There is a natural pairing between the two complexes C_θ and C_θ^\vee , by requiring the bases described above to be dual bases. This means that we consider as an identification the isomorphism

$$C_{j,\theta}^\vee \rightarrow \text{Hom}(C_{2-j,\theta}, \mathbb{Z})$$

whose image of $U_{i,a,\theta}[b]$ is dual to $S_{i,a,\theta}[b]$, and so on.

6.1.5. The inclusions eq. (6.1.4) are quasiisomorphisms. As a result, the homology groups of C_θ and C_θ^\vee are naturally isomorphic to the absolute and relative homology groups of A_θ^{inv} . Furthermore, the restriction of the pairing

$$\langle \cdot, \cdot \rangle : C_\theta \times C_\theta^\vee \rightarrow \mathbb{Z}$$

between C_θ and C_θ^\vee to cycles coincides with the natural pairing between cycles in $Z_j(A^{\text{inv}}; \mathbb{Z})$ and relative cycles in $Z_{2-j}(A^{\text{inv}}, \partial A^{\text{inv}}; \mathbb{Z})$.

6.2 The action on the chain complex

Having built the chain complex (C_θ, d_θ) in the previous section, we are now in a position to compute the algebraic monodromy. The geometric monodromy $G_\theta : A_\theta^{\text{inv}} \rightarrow A_\theta^{\text{inv}}$ (defined in [Definition 3.4.12](#)) is a diffeomorphism that permutes the trajectories of the flow ξ^{inv} in the periodic pieces and interpolates between them in the connecting annuli.

In this section, we compute the matrix B_θ of this action with respect to the basis of chains $\{S_{i,a,\theta}[b]\}$ defined previously. This matrix B_θ is the algebraic representation of the monodromy operator $(G_\theta)_*$ acting on the defined CW-complex of the fiber.

Action on $C_{0,\theta}$

We define $B_{0,\theta} : C_{0,\theta} \rightarrow C_{0,\theta}$ as the permutation matrix

$$\begin{pmatrix} 0 & 0 & 0 & \cdots & 1 \\ 1 & 0 & 0 & \cdots & 0 \\ 0 & 1 & 0 & \cdots & 0 \\ \vdots & \vdots & \vdots & \ddots & \vdots \\ 0 & 0 & 0 & \cdots & 0 \end{pmatrix}$$

of size $e = m_0$.

Action on $C_{1,\theta}$

We define the matrix $B_{1,\theta}$ acting on the chain complex as

$$B_{1,\theta} = (\langle G_\theta(S_{i,a,\theta}[b]), U_{i',a',\theta}[b'] \rangle)_{(i,a,b), (i',a',b') \in I_1}.$$

Here the intersection number is taken viewing $U_{i',a',\theta}[b]$ as a relative cycle in A_θ^{inv} relative to $\partial A_\theta^{\text{inv}}$, and $G_\theta(S_{i,a,\theta}[b])$ as a cycle in A_θ^{inv} relative to the set of points $q_{0,-1,\theta}[1], \dots, q_{0,-1,\theta}[e]$. We also recall that I_1 ([6.1.3](#)) is a totally ordered index set. Equivalently, $B_{1,\theta}$ is the linear operator $B_{1,\theta} : C_{1,\theta} \rightarrow C_{1,\theta}$ defined by

$$(6.2.1) \quad B_{1,\theta}(S_{i,a,\theta}[b]) = \sum_{(i',a',b') \in I_1} \langle G_\theta(S_{i,a,\theta}[b]), U_{i',a',\theta}[b'] \rangle S_{i',a',\theta}[b'].$$

We also give a name to some blocks of the matrix:

$$B_{1,i,\theta} = (\langle G_\theta(S_{i,a,\theta}[b]), U_{i',a',\theta}[b'] \rangle)_{(i,a,b), (i',a',b') \in I_{1,i}}$$

and

$$B_{1,i,a,\theta} = (\langle G_\theta(S_{i,a,\theta}[b]), U_{i',a',\theta}[b'] \rangle)_{(i,a,b), (i',a',b') \in I_{1,i,a}}$$

Next, we show the form that some of these blocks take.

Lemma 6.2.2. *The matrix $B_{1,\theta}$ is block upper triangular, with block diagonal entries the submatrices $B_{1,i,a,\theta}$.*

If $a \neq 0$, the matrix $B_{1,i,a,\theta}$ is the $m_i \times m_i$ permutation matrix

$$B_{1,i,a,\theta} = \begin{pmatrix} 0 & 0 & 0 & \cdots & 1 \\ 1 & 0 & 0 & \cdots & 0 \\ 0 & 1 & 0 & \cdots & 0 \\ \vdots & \vdots & \vdots & \ddots & \vdots \\ 0 & 0 & 0 & \cdots & 0 \end{pmatrix}$$

which is the companion matrix to the polynomial $t^{m_i} - 1$.

If $a = 0$, the matrix $B_{1,i,0,\theta}$ is the $(m_i - m_{ik}) \times (m_i - m_{ik})$ matrix of the form

$$B_{1,i,0,\theta} = \begin{pmatrix} -c_{m_i-m_{ik}-1} & -c_{m_i-m_{ik}-2} & \cdots & -c_1 & -c_0 \\ 1 & 0 & \cdots & 0 & 0 \\ 0 & 1 & \cdots & 0 & 0 \\ \vdots & \vdots & \ddots & \vdots & \vdots \\ 0 & 0 & \cdots & 1 & 0 \end{pmatrix}$$

which is the inverse transpose of the companion matrix to the polynomial

$$\frac{t^{m_i} - 1}{t^{m_{ik}} - 1} = \sum_{\ell=0}^{m_i-m_{ik}} c_\ell t^\ell = t^{m_i-m_{ik}} + t^{m_i-2m_{ik}} + t^{m_i-3m_{ik}} + \cdots + 1.$$

Furthermore, the matrix $B_{1,i,\theta}$ is the diagonal block matrix

$$B_{1,i,\theta} = \bigoplus_a B_{1,i,a,\theta}$$

Proof. For the first statement on the block upper triangular structure of $B_{1,\theta}$, first consider two distinct vertices i, k in Γ . The chain $S_{i,a,\theta}[b]$, as well as its image by G_θ is contained in the pieces

$$A_{\ell_0}^{\text{inv}}, A_{\ell_0, \ell_1}^{\text{inv}}, A_{\ell_1}^{\text{inv}}, \dots, A_{\ell_{s-1}, \ell_s}^{\text{inv}}, A_{\ell_s}^{\text{inv}}$$

where $0 = \ell_0 \rightarrow \ell_1 \rightarrow \dots \rightarrow \ell_s = i$ is the geodesic in Γ between 0 and i . Similarly, both prongs in $U_{k,c,\theta}[d]$ are contained in unions of pieces corresponding to directed geodesics in Γ starting at k . As a result, these cycles are disjoint, unless there is a directed geodesic starting at i and ending at k . Thus, the matrix $B_{1,\theta}$ is block upper triangular with diagonal blocks the matrices $B_{1,i,\theta}$. We will see below that these are block diagonal matrices with diagonal blocks $B_{1,i,a,\theta}$, proving the first statement.

This proof proceeds by analyzing the three statements of the lemma. The central element is the action of the monodromy map $G_\theta : A_\theta^{\text{inv}} \rightarrow A_\theta^{\text{inv}}$ on the chain complex $C_{1,\theta}$.

Proof of $B_{1,i,\theta} = \bigoplus_a B_{1,i,a,\theta}$ The intersection pairing $\langle \cdot, \cdot \rangle$ between a chain in A_i^{inv} and a chain in $A_{i'}^{\text{inv}}$ is zero unless $i = i'$. This implies $B_{1,\theta}$ is block-diagonal with respect to the vertex index i , i.e., $B_{1,\theta} = \bigoplus_i B_{1,i,\theta}$.

Furthermore, within A_i^{inv} , the map $G_\theta|_{A_i^{\text{inv}}} = G_{i,\theta}$ is the generator of the Galois group of the cover $\Pi_{i,\theta} : A_{i,\theta}^{\text{inv}} \rightarrow \hat{D}_i$. The map G_θ permutes the points of the finite fiber over any point $\hat{q} \in \hat{D}_i$. The chains $S_{i,a,\theta}[b]$ are stable manifolds of the singularities $q_{i,a,\theta}[b]$. The chain $U_{i,a',\theta}[b']$ is the unstable manifold of a singularity $q_{i,a',\theta}[b']$ in the fiber over $q_{i,a'} \in \hat{D}_i$. Thus, $G_\theta(S_{i,a,\theta}[b])$ is a chain that contains a point in the fiber over $q_{i,a}$ and similarly for the (relative) chain $U_{i,a',\theta}[b']$. Since G_θ sends trajectories to trajectories and singularities to singularities within the pieces $A_{i,\theta}^{\text{inv}}$, and since the sequences of vertices by which $U_{i,a',\theta}[b']$ passes and by which $S_{i,a,\theta}[b]$ passes only coincide at i , we deduce that the intersection pairing

$$\langle G_\theta(S_{i,a,\theta}[b]), U_{i,a',\theta}[b'] \rangle$$

can only be non-zero if their corresponding singularity lies over the same singularity of $\hat{\xi}$ in \hat{D}_i , which requires $a = a'$. Therefore, the matrix $B_{1,i,\theta}$ is itself block-diagonal with respect to the index a , proving the third statement of the lemma.

Proof for $a \neq 0$ (Saddle points) We now compute the block $B_{1,i,a,\theta}$ for $a \neq 0$. The relevant elements for this block are $\{S_{i,a,\theta}[b]\}_{b=1}^{m_i}$, and their corresponding duals are $\{U_{i,a,\theta}[b]\}_{b=1}^{m_i}$. The singularities $\{q_{i,a,\theta}[b]\}_{b=1}^{m_i}$ are the m_i saddle points which are preimages of the saddle point $q_{i,a} \in \hat{D}_i$ of $\hat{\xi}_i$. They are explicitly labeled by their α coordinates such that:

$$\alpha_i(q_{i,a,\theta}[b]) \in \left[\frac{2\pi(b-1)}{m_i}, \frac{2\pi b}{m_i} \right) + 2\pi\mathbb{Z}.$$

The monodromy map $G_\theta = G_{i,\theta}$ is the generator of this m_i -sheeted cyclic cover. Its action on the fiber corresponds to adding $\frac{2\pi}{m_i}$ to the α_i -coordinate. This action permutes cyclically the labeled points.

In particular, the action on the points is $G_\theta(q_{i,a,\theta}[b]) = q_{i,a,\theta}[b+1]$ (for $b < m_i$) and $G_\theta(q_{i,a,\theta}[m_i]) = q_{i,a,\theta}[1]$. By definition, G_θ maps the stable manifold of a point to the stable manifold of its image within the piece $A_{i,\theta}^{\text{inv}}$:

- ⌘ $G_\theta(S_{i,a,\theta}[b]) \cap A_{i,\theta}^{\text{inv}} = S_{i,a,\theta}[b+1] \cap A_{i,\theta}^{\text{inv}}$, for $b = 1, \dots, m_i - 1$.
- ⌘ $G_\theta(S_{i,a,\theta}[m_i]) \cap A_{i,\theta}^{\text{inv}} = S_{i,a,\theta}[1] \cap A_{i,\theta}^{\text{inv}}$.

The entries of the matrix $B_{1,i,a,\theta}$ are $(B)_{b',b} = \langle G_\theta(S_{i,a,\theta}[b]), U_{i,a,\theta}[b'] \rangle$.

- ⌘ For a column $b < m_i$: The entry is $\langle S_{i,a,\theta}[b+1], U_{i,a,\theta}[b'] \rangle = \delta_{b+1,b'}$. This gives a 1 in row $b+1$ and 0s elsewhere.
- ⌘ For the column $b = m_i$: The entry is $\langle S_{i,a,\theta}[1], U_{i,a,\theta}[b'] \rangle = \delta_{1,b'}$. This gives a 1 in row 1 and 0s elsewhere.

The resulting matrix is:

$$B_{1,i,a,\theta} = \begin{pmatrix} 0 & 0 & 0 & \cdots & 0 & 1 \\ 1 & 0 & 0 & \cdots & 0 & 0 \\ 0 & 1 & 0 & \cdots & 0 & 0 \\ \vdots & \vdots & \vdots & \ddots & \vdots & \vdots \\ 0 & 0 & 0 & \cdots & 1 & 0 \end{pmatrix}$$

This is the companion matrix for the polynomial $p(t) = t^{m_i} - 1$. For this polynomial, $n = m_i$, $c_0 = -1$, and $c_1 = \dots = c_{m_i-1} = 0$. The last column of the companion matrix is $(-c_0, -c_1, \dots, -c_{m_i-1})^T = (1, 0, \dots, 0)^T$. This matches our computed matrix (the 1 is in the first row, last column).

Proof for $a = 0$ (Multipronged singularities) For $a = 0$, we consider the block $B_{1,i,0,\theta}$. Let t be the variable representing the action of the monodromy G_θ . We first establish the structure of $C_{1,i,0,\theta}$ as a $\mathbb{Z}[t]$ -module.

The map $\Pi_{i,\theta} : A_{i,\theta}^{\text{inv}} \rightarrow \hat{D}_i$ is an m_i -sheeted cyclic cover. Let \hat{q} be a point in \hat{D}_i on the trajectory of $\hat{\xi}_i$ escaping from $q_{i,0}$ (on the positive axis). Let $C_{\text{fiber}}(\hat{q})$ denote the free \mathbb{Z} -module on the fiber $\Pi_{i,\theta}^{-1}(\hat{q})$.

- ⌘ The fiber over \hat{q} has m_i points. The module of unstable prongs $C_{\text{uprongs}} := C_{\text{fiber}}(\hat{q})$ is isomorphic to $\mathbb{Z}[t]/(t^{m_i} - 1)$ as a $\mathbb{Z}[t]$ -module.
- ⌘ For the singular point $q_{i,0}$ itself, the fiber has m_{ik} points. The module $C_{\text{points}} := C_{\text{fiber}}(q_{i,0})$ is isomorphic to $\mathbb{Z}[t]/(t^{m_{ik}} - 1)$.

There is a natural map $\phi : C_{\text{uprongs}} \rightarrow C_{\text{points}}$ that sends each prong to the singular point it converges to. This map is a surjective $\mathbb{Z}[t]$ -module homomorphism. The module $C_{1,i,0,\theta}$ is, by its construction from the prongs in [eq. \(6.1.1\)](#), precisely the kernel of this map, $\ker(\phi)$.

We have a short exact sequence of $\mathbb{Z}[t]$ -modules:

$$0 \rightarrow C_{1,i,0,\theta}^\vee \rightarrow C_{\text{uprongs}} \xrightarrow{\phi} C_{\text{points}} \rightarrow 0$$

Using the module isomorphisms, this becomes:

$$0 \rightarrow \ker(\phi) \rightarrow \mathbb{Z}[t]/(t^{m_i} - 1) \xrightarrow{\phi} \mathbb{Z}[t]/(t^{m_{ik}} - 1) \rightarrow 0$$

The kernel of the canonical projection ϕ is the ideal generated by $(t^{m_{ik}} - 1)$ inside the ring $\mathbb{Z}[t]/(t^{m_i} - 1)$. We thus have

$$C_{1,i,0,\theta}^\vee \cong \ker(\phi) = \frac{(t^{m_{ik}} - 1)}{(t^{m_i} - 1)} \subset \frac{\mathbb{Z}[t]}{(t^{m_i} - 1)}.$$

This kernel is a cyclic module generated by the element $g = (t^{m_{ik}} - 1)$. By the isomorphism theorem, this module is isomorphic to $\mathbb{Z}[t]/\text{Ann}(g)$, where $\text{Ann}(g)$ is the annihilator ideal of g in $\mathbb{Z}[t]$. A polynomial $P(t) \in \mathbb{Z}[t]$ is in $\text{Ann}(g)$ if $P(t) \cdot g = 0$ in the module $\mathbb{Z}[t]/(t^{m_i} - 1)$. This means

$$P(t) \cdot (t^{m_{ik}} - 1) \text{ is a multiple of } (t^{m_i} - 1) \text{ in } \mathbb{Z}[t].$$

Let $Q(t) = (t^{m_i} - 1)/(t^{m_{ik}} - 1)$. Since m_{ik} divides m_i , $Q(t)$ is a polynomial in $\mathbb{Z}[t]$. The condition becomes:

$$P(t) \cdot (t^{m_{ik}} - 1) = R(t) \cdot Q(t) \cdot (t^{m_{ik}} - 1) \quad \text{for some } R(t) \in \mathbb{Z}[t].$$

This implies $P(t)$ must be a multiple of $Q(t)$. The annihilator ideal is therefore $\text{Ann}(g) = (Q(t))$. We have thus shown:

$$C_{1,i,0,\theta}^\vee \cong \mathbb{Z}[t]/(Q(t)), \quad \text{where } Q(t) = \frac{t^{m_i} - 1}{t^{m_{ik}} - 1} = \sum_{\ell=0}^N c_\ell t^\ell,$$

and $N = m_i - m_{ik} = \deg(Q(t))$.

The basis $\{U_{i,0,\theta}[b]\}_{b=1}^N$ is, by construction (cf. [eq. \(6.1.1\)](#)), chosen to be a standard \mathbb{Z} -basis for this cyclic module, corresponding to $\{U[1], tU[1], t^2U[1], \dots, t^{N-1}U[1]\}$. Let $U[b] = U_{i,0,\theta}[b] \leftrightarrow t^{b-1}U[1]$. The action of G_θ (multiplication by t) is:

- ❀ For $b \in \{1, \dots, N-1\}$: $G_\theta(U[b]) = G_\theta(t^{b-1}U[1]) = t^bU[1] = U[b+1]$.
- ❀ For $b = N$: $G_\theta(U[N]) = G_\theta(t^{N-1}U[1]) = t^NU[1]$.

Since $U[1]$ is a generator and $Q(t) \cdot U[1] = 0$, we have:

$$(t^N + c_{N-1}t^{N-1} + \dots + c_1t + c_0)U[1] = 0$$

Solving for $t^NU[1]$, we get:

$$t^NU[1] = -c_{N-1}t^{N-1}U[1] - \dots - c_1tU[1] - c_0U[1]$$

Substituting back $U[b] = t^{b-1}U[1]$:

$$G_\theta(U[N]) = -c_{N-1}U[N] - \dots - c_1U[2] - c_0U[1]$$

Now we write the matrix $B_{1,i,0,\theta}^\vee$ whose entries are $(B)_{b',b} = \langle G_\theta(S[b]), U[b'] \rangle$.

- ❀ For a column $b < N$: $G_\theta(U[b]) = U[b+1]$. The column has a 1 in row $b+1$ and 0s elsewhere, since $\langle S[b+1], U[b'] \rangle = \delta_{b+1,b'}$.
- ❀ For the column $b = N$: $G_\theta(U[N]) = \sum_{\ell=0}^{N-1} -c_\ell U[\ell+1]$. The column vector is $(-c_0, -c_1, \dots, -c_{N-1})^T$.

This gives the matrix:

$$B_{1,i,0,\theta}^\vee = \begin{pmatrix} 0 & 0 & 0 & \cdots & 0 & -c_0 \\ 1 & 0 & 0 & \cdots & 0 & -c_1 \\ 0 & 1 & 0 & \cdots & 0 & -c_2 \\ \vdots & \vdots & \vdots & \ddots & \vdots & \vdots \\ 0 & 0 & 0 & \cdots & 1 & -c_{N-1} \end{pmatrix}$$

where $N = m_i - m_{ik}$. This is precisely the companion matrix for the polynomial $Q(t) = \sum_{\ell=0}^N c_\ell t^\ell$. Finally, $B_{1,i,0,\theta}^\vee = (B_{1,i,0,\theta}^{-1})^T$. ■

Notation 6.2.3. We denote by $B_\theta = B_{0,\theta} \oplus B_{1,\theta}$ the induced operator on $C_\theta = C_{0,\theta} \oplus C_{1,\theta}$ by the previously defined two operators.

6.3 Action on homology

Lemma 6.3.1. *The operator B_θ acts on the complex (C_θ, d_θ) . And the induced map on homology coincides with the map $(G_\theta)_*$ induced on homology by the geometric monodromy G_θ .*

Proof. First observe that the action of $B_{0,\theta}$ and G_θ on the points that generate $C_{0,\theta}$ coincides. Denote the set of these points by S_0 in this proof. On one hand this implies that $(G_\theta)_*$ acts on the relative homology group $H_1(A_\theta^{\text{inv}}, S_0; \mathbb{Z})$. On the other hand, we have the sequence of isomorphisms $H_1(A_\theta^{\text{inv}}, S_0; \mathbb{Z}) \simeq \tilde{H}_1(A_\theta^{\text{inv}}/S_0; \mathbb{Z}) \simeq C_{1,\theta}$. So we are left to prove that the actions of $B_{1,\theta}$ on $C_{1,\theta}$ and $(G_\theta)_*$ on $H_1(A_\theta^{\text{inv}}, S_0; \mathbb{Z})$ coincide via the above isomorphisms. But this follows from the construction of $B_{1,\theta}$ in eq. (6.2.1) and the definition of $(G_\theta)_*$. ■

This lemma confirms that our algebraic construction B_θ faithfully represents the topological monodromy. We now turn to the other principal invariant, the variation operator.

7 Description of the variation operator

In the previous section, we analyzed the action of the monodromy G_θ . In this section, we describe the second key topological invariant: the variation operator. The classical variation operator, $\text{Var} : H_1(A_\theta^{\text{inv}}, \partial A_\theta^{\text{inv}}; \mathbb{Z}) \rightarrow H_1(A_\theta^{\text{inv}}; \mathbb{Z})$, measures the difference between a relative cycle and its image under the monodromy.

We will define a chain-level operator $V : C_{1,\theta}^\vee \rightarrow C_{1,\theta}$ that acts between our dual complex and the primary complex. As shown in Lemma 7.2.1, this operator V is the realization on the chain complex of the classical variation operator.

7.1 V on the chain complex

We define the operator $V : C_{1,\theta}^\vee \rightarrow C_{1,\theta}$ by the formula

$$(7.1.1) \quad V_{1,\theta}(U_{i,a,\theta}[b]) = \sum_{(i',a',b') \in I_1} \langle G_\theta(U_{i,a,\theta}[b]) - U_{i,a,\theta}[b], U_{i',a',\theta}[b'] \rangle S_{i',a',\theta}[b'].$$

Note that since G_θ equals the identity map on $\partial A_\theta^{\text{inv}}$, then $G_\theta(U_{i,a,\theta}[b]) - U_{i,a,\theta}[b]$ is an absolute cycle and the intersection product of the formula above is well defined.

7.2 Var on homology

By a similar argument as the one in [Lemma 6.3.1](#), we get

Lemma 7.2.1. *The linear operator V defines a map $H_1(A_\theta^{\text{inv}}, \partial A_\theta^{\text{inv}}; \mathbb{Z}) \rightarrow H_1(A_\theta^{\text{inv}}; \mathbb{Z})$ which coincides with the classical variation operator.*

Proof. We first show V induces a map on homology $V_* : H_1(C_\theta^\vee) \rightarrow H_1(C_\theta)$.

(i) **V maps relative cycles to absolute cycles:** Let $U \in Z_{1,\theta}^\vee$ (so $\partial U = 0$). The chain $V(U) = G_\theta(U) - U$ is an absolute cycle because G_θ acts as the identity on $\partial A_\theta^{\text{inv}}$, which contains the boundary of U . So,

$$\partial(V(U)) = \partial(G_\theta(U) - U) = \partial(G_\theta(U)) - \partial U = G_\theta(\partial U) - \partial U = G_\theta(0) - 0 = 0.$$

So $V(U) \in Z_{1,\theta}$.

(ii) **V maps relative boundaries to absolute boundaries:** Let $U \in B_{1,\theta}^\vee$, so $U = \partial^\vee W$ for some $W \in C_{2,\theta}^\vee$. Since G_θ commutes with ∂ :

$$V(U) = G_\theta(\partial^\vee W) - \partial^\vee W = \partial(G_\theta(W)) - \partial W = \partial(G_\theta(W) - W).$$

Since $G_\theta(W) - W$ is an absolute 2-chain, $V(U)$ is an absolute 1-boundary.

Therefore, V descends to a well-defined homomorphism $V_* : H_1(C_\theta^\vee) \rightarrow H_1(C_\theta)$ given by $V_*([U]) = [G_\theta(U) - U]$.

Next, we show this map coincides with the classical variation operator, $\text{Var}_{\text{classic}}$. The inclusions $C_\theta^\vee \hookrightarrow C(A_\theta^{\text{inv}}, \partial A_\theta^{\text{inv}})$ and $C_\theta \hookrightarrow C(A_\theta^{\text{inv}})$ are quasi-isomorphisms, inducing isomorphisms on homology:

$$\begin{aligned} \Psi : H_1(C_\theta^\vee) &\xrightarrow{\cong} H_1(A_\theta^{\text{inv}}, \partial A_\theta^{\text{inv}}) \\ \Phi : H_1(C_\theta) &\xrightarrow{\cong} H_1(A_\theta^{\text{inv}}) \end{aligned}$$

The operator V from the lemma is the map $\text{Var}_{\text{lemma}} = \Phi \circ V_* \circ \Psi^{-1}$. The classical operator is $\text{Var}_{\text{classic}}([c]) = [G_\theta(c) - c]$.

Let $[c] \in H_1(A_\theta^{\text{inv}}, \partial A_\theta^{\text{inv}})$ be an arbitrary class. Let $[U] = \Psi^{-1}([c])$ be its corresponding class in $H_1(C_\theta^\vee)$. The chain U is thus a representative cycle for $[c]$.

⌘ Applying $\text{Var}_{\text{lemma}}$:

$$\text{Var}_{\text{lemma}}([c]) = (\Phi \circ V_* \circ \Psi^{-1})([c]) = \Phi(V_*([U])) = \Phi([G_\theta(U) - U]) = [G_\theta(U) - U].$$

⌘ Applying $\text{Var}_{\text{classic}}$:

$$\text{Var}_{\text{classic}}([c]) = [G_\theta(U) - U].$$

Since both maps yield the same absolute homology class $[G_\theta(U) - U] \in H_1(A_\theta^{\text{inv}})$, they are identical. ■

8 Gyrographs

8.0.1. In this section, we provide a method which can simplify the direct calculation of the matrices for monodromy and variation map. If θ is a generic angle, then the invariant spine S_θ^{inv} naturally has the structure of a conformal ribbon graph, being embedded in a surface, where near the vertices, we have a natural conformal structure. This data, together with the Hironaka numbers, allow us to calculate by hand the variation map for plane curve singularities.

8.1 A general construction

8.1.1. We denote by S a graph, with vertex set \mathcal{V} and edge set \mathcal{E} . We will assume that every edge has two distinct adjacent vertices, i.e. there are no loops, but we do allow for multiple edges joining the same pair of vertices. Denote by \mathcal{E}_v the set of edges adjacent to a vertex $v \in \mathcal{V}$. A *ribbon graph* structure on S allows us to define safe walks in S . Recall that a safe walk is a path on the ribbon graph that turns right at each vertex, see [A'C10]. To allow for flexibility, we do not always make an explicit distinction between a graph, and its topological realization. Throughout, we will consider a special subset of vertices $\mathcal{R} \subset \mathcal{V}$ in S . We will assume that any edge in S does not have both its vertices in \mathcal{R} , a condition that holds for the invariant spine, with all singularities seen as vertices. In general, we can subdivide any such edge in two by adding a vertex not in \mathcal{R} , to avoid any problems.

Definition 8.1.2. A *conformal ribbon graph* is a graph S , along with angles $a_v(e, f) \in \mathbb{R}/2\pi\mathbb{Z}$ associated to any pair of edges e, f adjacent to any vertex v in S , satisfying

$$a_v(e, g) = a_v(e, f) + a_v(f, g), \quad a_v(e, f) \neq 0 \quad \text{if } e \neq f$$

for any edge g also adjacent to v . At any vertex $v \in \mathcal{V}$ we have an $\mathbb{R}/2\pi\mathbb{Z}$ -torsor Θ_v , given as

$$\coprod_{e \in \mathcal{E}_v} \{e\} \times (\mathbb{R}/2\pi\mathbb{Z}) / \sim, \quad (e, \alpha) \sim (f, \alpha + a_v(e, f)), \quad e, f \in \mathcal{E}_v.$$

For any $\mathcal{R} \subset \mathcal{V}$, we set

$$\Theta_{\mathcal{R}} = \coprod_{r \in \mathcal{R}} \Theta_r$$

Definition 8.1.3. Let S be a conformal ribbon graph, and let $\mathcal{R} \subset \mathcal{V}$ be a set of vertices. The real oriented blow-up $\text{Bl}_{\mathcal{R}}^{\text{ro}}(S)$ of S at \mathcal{R} is the topological space given as the disjoint union of the sets $\Theta_{\mathcal{R}}$ and $\mathcal{V} \setminus \mathcal{R}$, with topology gluing the end points of any edge to the corresponding angle in $\Theta_{\mathcal{R}}$, if the endpoint is in \mathcal{R} .

Definition 8.1.4. Let S be a conformal ribbon graph. A *gyration* δ of angle $\lambda \in \mathbb{R}$ around \mathcal{R} in S is a continuous path in $\text{Bl}_{\mathcal{R}}^{\text{ro}}(S)$ satisfying the following conditions:

- ⌘ The starting and finishing points of δ are in $\Theta_{\mathcal{R}}$.
- ⌘ The combined length of all the segments of δ which are contained in $\Theta_{\mathcal{R}}$ add up to λ , and the path is oriented according to the orientation of $\Theta_{\mathcal{R}}$ along these segments.
- ⌘ Any segment of δ outside $\Theta_{\mathcal{R}}$ is a safe walk.

The *induced path* in S is the projection of this path to S , seen as a path in a graph.

8.1.5. Given a gyration δ , we say that time passes with speed 1 along segments of $\Theta_{\mathcal{R}}$, whereas safe paths in its complement are taken instantaneously. Thus, time passes from 0 to λ along a gyration of angle λ . Assume that the gyration δ passes through the angle of an edge in S adjacent to $r \in \mathcal{R}$ at time t , such that just before t , the path is on $\Theta_{\mathcal{R}}$. There are then two possibilities. After time t , the path proceeds along a safe path in $\text{Bl}_{\mathcal{R}}^{\text{ro}}(S)$, until it comes back to $\Theta_{\mathcal{R}}$, in which case we say that the gyration *takes a turn* along the corresponding edge, or the path proceeds along $\Theta_{\mathcal{R}}$, in which case we say that the path *ignores the turn*. Thus, a gyration can be constructed by specifying a starting or a finishing point in $\text{Bl}_{\mathcal{R}}^{\text{ro}}(S)$, along with instructions on which turns to take, and which ones to ignore, along the way.

8.1.6. Let S be a conformal ribbon graph, with $\mathcal{R} \subset \mathcal{V}$. Let P be the graph obtained from $\text{Bl}_{\mathcal{R}}^{\text{ro}}(S)$ by deleting edges contained in $\Theta_{\mathcal{R}}$. Consider data of the following form:

- (i) Nonnegative real weights $\varsigma_C, \varsigma_C^\vee \in \mathbb{R}_{\geq 0}$ associated with every component C of P . For a vertex or edge v, e in C , we set $\varsigma_v = \varsigma_e = \varsigma_C$. and $\varsigma_v^\vee = \varsigma_e^\vee = \varsigma_C^\vee$.
- (ii) An S^1 -invariant bijective map $k_\Theta : \Theta_{\mathcal{R}} \rightarrow \Theta_{\mathcal{R}}$, inducing a permutation $k_{\mathcal{R}} : \mathcal{R} \rightarrow \mathcal{R}$.
- (iii) An automorphism k_P of the ribbon graph P .

For any edge e in S adjacent to $r \in \mathcal{R}$ and $v \in \mathcal{V} \setminus \mathcal{R}$, we define gyrations as follows.

- ⌘ The *absolute* gyration δ_e has length ς_e , starts at $k_P(e)$ in Θ_r , and takes a turn along an edge f at time t if and only if $t > \varsigma_e - \varsigma_f$.
- ⌘ The *relative* gyration δ_e^\vee has length ς , starts at e , and takes a turn along an edge f at time t if and only if $t > \varsigma_f^\vee - \varsigma_e^\vee$.

Definition 8.1.7. A conformal ribbon graph S and $\mathcal{R} \subset \mathcal{V}$ a set of vertices, along with weights ς_i on its vertices, constant along connected components of $S \setminus \mathcal{R}$, is a *gyrograph* if, for every edge e in S , adjacent to $r \in \mathcal{R}$ and $v \in \mathcal{V} \setminus \mathcal{R}$, the following hold for any edge e in S , adjacent to $r \in \mathcal{R}$

- ⌘ **The absolute gyrograph property:** the absolute gyration δ_e ends at $k_\Theta(e)$.
- ⌘ **The relative gyrograph property:** Let s be an interior point of some edge in S , and consider a safe walk starting at s , stopping as soon as we reach \mathcal{R} , having final edge f . Then, the relative gyration δ_f^\vee ends at some edge of S , and a safe walk which starts following this edge, finds $k_P(s)$ before returning to \mathcal{R} .

Definition 8.1.8. Given a gyrograph S , with the notation introduced in 8.1.6, we can define a continuous map

$$(8.1.9) \quad k_S : S \rightarrow S$$

up to homotopy, as follows. For any $r \in \mathcal{R}$, we set $k_S(r) = k_{\mathcal{R}}(r)$, and if $v \in \mathcal{V} \setminus \mathcal{R}$, then $k_S(v) = k_P(v)$. For any e in S , the path $k_S(e)$ in S is the concatenation of $k_P(e)$ and the path induced by the gyration δ_e . The absolute condition in Definition 8.1.7 guarantees that this way, k_S is a continuous map. We call this element of $[S, S]$ the *monodromy spoor* of S .

Now, let e be any edge in S , with some orientation. Denote by e^\vee an oriented dual segment to the edge e in a thickening F of S . That is, the segment e^\vee intersects S in a single point $s \in e$, an interior point of e , this intersection is transverse, and the intersection number of e and e^\vee at s is $+1$. Let w_+ be the concatenation of the safe walk from s along the chosen orientation, the relative gyration defined by the last edge of this walk, and then a safe walk which finds $k_P(s)$, and define w_- similarly, starting the safe walk against the chosen orientation. We then have an oriented cycle $w_+ - w_-$, which we denote by v_e , and call the *variation spoor* of e , as in [A'C18, Section 6].

8.2 The invariant spine as a gyrograph

8.2.1. In this subsection, we put a gyrograph structure on the invariant spine $S = S_\theta^{\text{inv}}$, for a generic angle θ . Recall Definition 5.2.1 for the definition of the Hironaka number.

Definition 8.2.2. Let θ be a generic angle for the f as in Definition 5.1.1. With $S = S_\theta^{\text{inv}}$ the invariant spine of f , denote by $\mathcal{V} = \mathcal{V}_\theta$ the set of singularities of ξ_θ^{ro} , and \mathcal{E} the set of trajectories, forming a graph. Let $\mathcal{R} = \mathcal{R}_\theta \subset \mathcal{V}_\theta$ be the set of vertices corresponding to the repellers $q_{0,-1,\theta}[1], \dots, q_{0,-1,\theta}[m_0]$. As this graph is embedded in A_θ^{inv} , which has a conformal structure near the vertices, it inherits a conformal structure. In particular, the set $\Theta_{\mathcal{R}}$ is naturally seen as a subset of the coordinate space $\{(\tilde{\alpha}_0, \tilde{\beta}_0)\}$, with $\mathbb{R}/2\pi\mathbb{Z}$ acting on the $\tilde{\beta}_0$ coordinate,

$$\Theta_{\mathcal{R}} = \left\{ (\tilde{\alpha}_0, \tilde{\beta}_0) \in (\mathbb{R}/2\pi\mathbb{Z})^2 \mid m_0\alpha_0 = \theta \right\}.$$

For any vertex $v = q_{i,a,\theta}[b] \in \mathcal{V}_\theta \setminus \mathcal{R}_\theta$, set

$$\varsigma_v = h_0^{-1} - h_i^{-1}, \quad \varsigma_v^\vee = h_i^{-1}.$$

We define a map $k_\Theta : \Theta_R \rightarrow \Theta_R$ by

$$(\tilde{\alpha}_0, \tilde{\beta}_0) \mapsto \left(\tilde{\alpha}_0 + \frac{1}{m_0}, \tilde{\beta}_0 \right).$$

Using the notation in [Section 6](#), we define a graph automorphism k_P by

$$q_{i,0,\theta}[c] \mapsto q_{i,a,\theta}[c+1], \quad c \in \mathbb{Z}/m_{ik}\mathbb{Z}$$

and

$$q_{i,a,\theta}[b] \mapsto q_{i,a,\theta}[b+1], \quad b \in \mathbb{Z}/m_i\mathbb{Z}$$

for $a > 0$. For prongs, and any a , we map

$$P_{i,0,\theta}[b] \mapsto P_{i,0,\theta}[b+1], \quad P_{i,a,\theta}^\pm[b] \mapsto P_{i,a,\theta}^\pm[b+1], \quad b \in \mathbb{Z}/m_i\mathbb{Z}.$$

Theorem 8.2.3. *The invariant spine S_θ^{inv} , with the data in [Definition 8.2.2](#) is a gyrograph. Furthermore, the monodromy spoor of S_θ^{inv} coincides with the homotopy class of the geometric monodromy, and if $e \in \mathcal{E}_\theta$ is an edge, and e^\vee is a dual edge to it, then the variation spoor v_e of e coincides with the variation map of e^\vee .*

Proof. Let $i, k \in \mathcal{V}$ be vertices in Γ joined by an edge $i \rightarrow k$, and assume that there is an edge $j \rightarrow i$. If $i = 0$, then we use the virtual vertex $j = -1$. The map $\Delta_{ik} : D_{ik}^{\text{ro}} \dashrightarrow D_{ji}^{\text{ro}}$ has constant Jacobian matrix with respect to the coordinates $(\tilde{\alpha}_k, \tilde{\beta}_k)$ and $(\tilde{\alpha}_i, \tilde{\beta}_i)$. Denote this matrix by K_k . Using [Lemmas 3.5.10](#) and [5.0.3](#), and the changes of variables

$$(\tilde{\alpha}_i, \tilde{\beta}_i) = (\alpha_i + b_i \beta_i, -\beta_i), \quad (\alpha_i, \beta_{ik}) = (\tilde{\beta}_k, \tilde{\alpha}_k),$$

we find

$$K_k = \begin{pmatrix} 1 & b_i \\ 0 & -1 \end{pmatrix} \begin{pmatrix} 1 & \frac{m_k}{m_i} + \left(\frac{m_j}{m_i} - b_i \right) \frac{n_{ik}}{n_{ij}} \\ 0 & \frac{n_{ik}}{n_{ij}} \end{pmatrix} \begin{pmatrix} 0 & 1 \\ 1 & 0 \end{pmatrix} = \begin{pmatrix} \frac{m_k}{m_i} + \frac{m_j}{m_i} \frac{n_{ik}}{n_{ij}} & 1 \\ -\frac{n_{ik}}{n_{ij}} & 0 \end{pmatrix}.$$

Let P be a trajectory in A^{inv} , and consider its image under G . If P passes through A_i^{inv} , then this part of the trajectory is mapped to another trajectory passing through A_i^{inv} . If P passes through A_{ik}^{inv} , then its image in A^{inv} makes a turn by the vector $-w_k/(m_i m_k)$, where we set

$$w_k = 2\pi \begin{pmatrix} m_i \\ -m_k \end{pmatrix}$$

in the coordinates $(\tilde{\alpha}_k, \tilde{\beta}_k)$ in A_{ik}^{inv} , and then continues as a trajectory in A_i^{inv} . Now, a direct computation gives

$$K_k w_k = \frac{n_{ik}}{n_{ji}} w_i.$$

Consider the unique geodesic $0 \rightarrow i_1 \rightarrow \dots \rightarrow i_{l-1} \rightarrow i_l$ with $i_0 = 0$, $i_{l-1} = i$ and $i_l = k$ in the graph Γ . Then, the above formula gives a telescopic product

$$K_{i_1} \cdots K_{i_{l-1}} K_{i_l} \frac{w_k}{m_i m_k} = \frac{n_{ik}}{m_i m_k n_{-1,0}} w_0 = \frac{2\pi n_{ik}}{m_i m_k n_{-1,0}} \begin{pmatrix} 0 \\ -m_0 \end{pmatrix} = \frac{n_{ik}}{m_i m_k} \begin{pmatrix} 0 \\ -2\pi \end{pmatrix}.$$

Assume now that the turn that the image of P makes in A_{ik}^{inv} does not cross any unstable manifold. Then, by applying the backwards flow of ξ^{inv} to this turn, we can see this as a

gyration by $-2\pi n_{ik}/(m_i m_k)$ radians around a repeller. If the image does cross an unstable manifold, then, applying backwards flow by ξ^{inv} to the turn in A_{ik}^{inv} ends up in a the same total gyration around repellers, with fast jumps along safe paths in between.

If P is a stable prong with an end point in a singularity of ξ^{inv} in $D_{k,\theta}^{\text{ro}}$, say $P = P_{k,a,\theta}^{\pm}[b]$ for some a, b , apply backwards flow to the whole of $G(P)$ (see [Definition 3.4.4](#) for notation). We end up with a total gyration around repellers by an angle

$$-2\pi \sum_{s=1}^l \frac{n_{i_{s-1}i_s}}{m_{i_{s-1}}m_{i_s}} = -2\pi \sum_{s=1}^l \frac{c_{0,i_{s-1}}}{m_{i_{s-1}}} - \frac{c_{0,i_s}}{m_{i_s}} = h_k^{-1} - h_0^{-1} = -\varsigma_k.$$

As a result, if e is the edge in S_θ^{inv} corresponding to the prong $P = P_{k,a,\theta}^{\pm}[b]$, then the image $G(P)$ is isotopic (fixing the end points) to the composition of the prong $P_{k,a,\theta}^{\pm}[b+1]$ and a gyraton of length ς_k . This is precisely the gyration δ_e . Indeed, assume that we encounter another edge e' in the spine S_θ^{inv} along the gyration at time t , and that this edge e' corresponds to some prong $P' = P_{\ell,c,\theta}[d]$. There exists a unique s such that

$$\varsigma_k - \varsigma_{i_s} < t < \varsigma_k - \varsigma_{i_{s-1}}.$$

If $\varsigma_\ell \geq \varsigma_{i_s}$, i.e. if $\varsigma_\ell > \varsigma_k - t$, then $G(P)$ already crosses the prong P' , and the gyration ignores the turn. Otherwise, the gyration takes the turn.

As a result, we conclude that the data in [Definition 8.2.2](#) satisfies the absolute gyrograph property. Indeed, this follows from the fact that the composition of the prong $P_{k,a,\theta}[b+1]$ and the gyration obtained from $G(P_{k,a,\theta}[b])$ is well defined.

Now, the relative gyrograph property is proved similarly. We start by considering a singularity $q_{i,a,\theta}[b]$. Let $j_0 \rightarrow j_1 \rightarrow \dots \rightarrow j_r$ with $j_0 = k$, be the path induced by the prong $R_{i,a,\theta}^+[b]$, ending in some arrowhead vertex $a = j_r$. Using a similar argument as above, using backwards flow of ξ^{inv} , shows that $G(R_{i,a,\theta}^+)$ is isotopic to the concatenation of $R_{i,a,\theta}^+[b]$, then a safe walk from $q_{i,a,\theta}[b]$ until we reach \mathcal{R}_θ , then a gyration, and then a safe walk which reaches $q_{i,a,\theta}[b+1]$, and does not pass through \mathcal{R}_θ . This gyration has angle

$$\sum_{s=0}^{r-1} h_{j_s}^{-1} - h_{j_{s+1}}^{-1} = h_i^{-1} = \varsigma_v^\vee$$

since $h_{j_r}^{-1} = 0$, as j_r is an arrowhead vertex. That this composition of paths is allowed proves the relative gyrograph property of this data.

It follows from this construction that the image by G_θ of any edge is homotopic to the path which defines the monodromy spoor, relative to its end-points. As a result, the monodromy spoor is the homotopy type of the geometric monodromy.

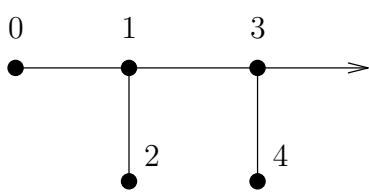
Furthermore, applying the variation map of G_θ to a dual edge e^\vee gives precisely the variation spoor v_e . ■

8.3 An example with two Puiseux-pairs

8.3.1. Let us use the gyrograph structure on S_θ^{inv} to calculate the algebraic monodromy and variation map of the simplest branch having two Puiseux pairs, given by the equation

$$f(x, y) = (y^2 - x^3)^2 + x^5 y.$$

The minimal embedded resolution graph of f , along with data, is as follows.



i	$-b_i$	$c_{0,i}$	m_i	h_i	ς_i	ς_i^\vee
0	-3	1	4	4	0	1/4
1	-2	2	12	6	1/12	1/6
2	-3	1	6	6	1/12	1/6
3	-1	4	26	13/2	5/52	2/13
4	-2	2	13	13/2	5/52	2/13

The gyrograph has four repellers $\mathcal{R} = \{q_{0,-1,\theta}[1], q_{0,-1,\theta}[2], q_{0,-1,\theta}[3], q_{0,-1,\theta}[4]\}$, as well as two groups of vertices

$$q_{1,0,\theta}[1], \dots, q_{1,0,\theta}[6], \quad q_{3,0,\theta}[1], \dots, q_{3,0,\theta}[13],$$

each permuted cyclically by the monodromy. In [fig. 8.3.1](#) we see these vertices, along with green and blue stable prongs, but with the repellers removed, whereas in [fig. 8.3.2](#) we see a neighborhood of $\Theta_{\mathcal{R}}$ in the blown up graph $\text{Bl}_{\mathbb{R}}^{\text{ro}}(S_{\theta}^{\text{inv}})$, as well as the 12 blue prongs coming from the first set of vertices, and the 26 green prongs coming from the second set of vertices. The action on $\Theta_{\mathcal{R}}$ is induced by the explicit map G_0 acting on a neighborhood of the repellers, in \tilde{U}_0 . In [fig. 8.3.2](#), it sends each boundary component cyclically to the next one to the right. By choosing coordinates, we can assume that any point is the end point of a blue prong. We label that prong by 1, and the rest of the prongs are labelled cyclically, using the monodromy near the vertices $q_{1,0,\theta}[b]$. The location of the rest of the blue prongs is then determined, since the end-point of the next blue prong is found by moving one step to the right, and going backwards by a gyration of length $\varsigma_2 = 1/12$. This gyration takes no turns. Now, choose any point on $\Theta_{\mathcal{R}}$

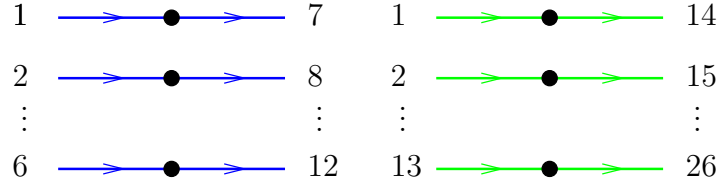


Figure 8.3.1: The spine S_{θ}^{inv} , with repellers removed, and stable prongs labelled cyclically. The black dots are the points $q_{i,0,\theta}[b]$.

which is not the endpoint of a blue prong. Then there exists some θ such that this is the end point of a green prong. We label this prong by 1, and the rest cyclically as above. The rest of the green prongs, and their cyclic order is then determined, again by jumping to the right, from any green prong, and following a gyration of length

$$\varsigma_4 = \frac{1}{4} - \frac{2}{13} = \frac{5}{52}$$

backwards, with the rule that if a blue prong is encountered at time

$$t < \frac{5}{52} - \frac{1}{12} = \frac{1}{78}$$

then we make a turn, otherwise the turn is ignored. In figure [fig. 8.3.2](#), we have chosen a green prong at a point near the first blue prong, so that the gyration starting at the first green prong of length $5/52$ takes a turn along blue prong number 1, comes back at the blue prong number 7, and meets up with the image of the green prong number 26 under k_{Θ} in Θ_{r_3} .

Clearly, we have

$$B_{0,\theta} = \begin{pmatrix} 0 & 0 & 0 & 1 \\ 1 & 0 & 0 & 0 \\ 0 & 1 & 0 & 0 \\ 0 & 0 & 1 & 0 \end{pmatrix}$$

Choosing a suitable orientation in [fig. 8.3.1](#), and using [fig. 8.3.2](#), we find that the differential $d_{1,\theta}$ is given by the matrix

$$\left(\begin{array}{cccccc|cccccccccccc} -1 & 0 & 1 & 0 & -1 & 0 & -1 & 0 & 0 & 1 & -1 & 0 & 0 & 1 & -1 & 0 & 0 & 1 & -1 \\ 0 & -1 & 0 & 1 & 0 & -1 & 1 & -1 & 0 & 0 & 1 & -1 & 0 & 0 & 1 & -1 & 0 & 0 & 1 \\ 1 & 0 & -1 & 0 & 1 & 0 & 0 & 1 & -1 & 0 & 0 & 1 & -1 & 0 & 0 & 1 & -1 & 0 & 0 \\ 0 & 1 & 0 & -1 & 0 & 1 & 0 & 0 & 1 & -1 & 0 & 0 & 1 & -1 & 0 & 0 & 1 & -1 & 0 \end{array} \right)$$

From what we have seen, the map k_S , with $S = S_\theta^{\text{inv}}$, permutes the blue prongs cyclically. The green prongs are similarly permuted cyclically, with the exception that the prong labelled by 26 is mapped to prong 1, and then blue prong 1 and 7. Taking the segment in [fig. 8.3.1](#) as a basis for $C_{1,\theta}$, we find that $B_{1,\theta}$ is a block matrix. Along the diagonal, we have matrices of size 6×6 and 13×13 which are similar to permutation matrices, but have a -1 in the corner, since applying the monodromy 6 times to a blue segment returns it to itself with the opposite orientation, and similarly for green segments. In the upper off-diagonal block we have one nonzero entry, the rest is zero. Indeed, the only turn taken by an absolute gyrations is that of the green prong 26, which turns along prong 7, and then follows prong 1, to come back to green prong 1. Taking into account orientation, this gives a -1 in the upper right hand corner.

$$B_{1,\theta} = \left(\begin{array}{cccccc|cccccccccccc} 0 & 0 & 0 & 0 & 0 & -1 & 0 & 0 & 0 & 0 & 0 & 0 & 0 & 0 & 0 & 0 & 0 & -1 \\ 1 & 0 & 0 & 0 & 0 & 0 & 0 & 0 & 0 & 0 & 0 & 0 & 0 & 0 & 0 & 0 & 0 & 0 \\ 0 & 1 & 0 & 0 & 0 & 0 & 0 & 0 & 0 & 0 & 0 & 0 & 0 & 0 & 0 & 0 & 0 & 0 \\ 0 & 0 & 1 & 0 & 0 & 0 & 0 & 0 & 0 & 0 & 0 & 0 & 0 & 0 & 0 & 0 & 0 & 0 \\ 0 & 0 & 0 & 1 & 0 & 0 & 0 & 0 & 0 & 0 & 0 & 0 & 0 & 0 & 0 & 0 & 0 & 0 \\ 0 & 0 & 0 & 0 & 1 & 0 & 0 & 0 & 0 & 0 & 0 & 0 & 0 & 0 & 0 & 0 & 0 & 0 \\ \hline 0 & 0 & 0 & 0 & 0 & 0 & 0 & 0 & 0 & 0 & 0 & 0 & 0 & 0 & 0 & 0 & 0 & -1 \\ 0 & 0 & 0 & 0 & 0 & 0 & 1 & 0 & 0 & 0 & 0 & 0 & 0 & 0 & 0 & 0 & 0 & 0 \\ 0 & 0 & 0 & 0 & 0 & 0 & 0 & 1 & 0 & 0 & 0 & 0 & 0 & 0 & 0 & 0 & 0 & 0 \\ 0 & 0 & 0 & 0 & 0 & 0 & 0 & 0 & 1 & 0 & 0 & 0 & 0 & 0 & 0 & 0 & 0 & 0 \\ 0 & 0 & 0 & 0 & 0 & 0 & 0 & 0 & 0 & 1 & 0 & 0 & 0 & 0 & 0 & 0 & 0 & 0 \\ 0 & 0 & 0 & 0 & 0 & 0 & 0 & 0 & 0 & 0 & 1 & 0 & 0 & 0 & 0 & 0 & 0 & 0 \\ 0 & 0 & 0 & 0 & 0 & 0 & 0 & 0 & 0 & 0 & 0 & 1 & 0 & 0 & 0 & 0 & 0 & 0 \\ 0 & 0 & 0 & 0 & 0 & 0 & 0 & 0 & 0 & 0 & 0 & 0 & 1 & 0 & 0 & 0 & 0 & 0 \\ 0 & 0 & 0 & 0 & 0 & 0 & 0 & 0 & 0 & 0 & 0 & 0 & 0 & 1 & 0 & 0 & 0 & 0 \\ 0 & 0 & 0 & 0 & 0 & 0 & 0 & 0 & 0 & 0 & 0 & 0 & 0 & 0 & 1 & 0 & 0 & 0 \\ 0 & 0 & 0 & 0 & 0 & 0 & 0 & 0 & 0 & 0 & 0 & 0 & 0 & 0 & 0 & 1 & 0 & 0 \\ 0 & 0 & 0 & 0 & 0 & 0 & 0 & 0 & 0 & 0 & 0 & 0 & 0 & 0 & 0 & 0 & 1 & 0 \end{array} \right)$$

Now, let us calculate the variation map $V_{1,\theta}$ in this basis, and its dual. If e is a blue prong, then the relative gyration δ_e^\vee starts at the edge e and takes a turn along any green edge, if it is encountered at time

$$t < \varsigma_1^\vee - \varsigma_3^\vee = \frac{1}{6} - \frac{2}{13} = \frac{1}{78}$$

This is what happens if e is the first blue prong. The relative gyration finds the green prong 21, makes a fast safe walk to green prong 8, and then stops at blue prong 8. From there, there is a safe walk to $k_P(e)$, i.e. blue prong 2. To construct v_e , we must also consider the other gyration, following a safe walk from blue prong 1 to blue prong 7, then a gyration of length $1/6$ which makes a turn at green prong 15, and then finishes gyrating from green prong 2 to blue prong 2. This shows that the cycle v_e induces the homological cycle given by the first column in the matrix $V_{1,\theta}$ below. This includes the first entries of the column equal to 1, since v_e crosses the blue prong 1, and its image by k_P , i.e. blue prong 2. It also makes two green jumps, which, by the orientation indicated,

If e is a green prong, then the relative gyration δ_e^\vee always makes a turn if it encounters a blue edge. In this example, we see that this gyration actually never encounters another green edge. If e is the first green edge, then v_e is the cycle which starts at e , makes a turn at the blue edge labelled 1 and makes a quick safe walk to the blue edge labelled 7, and continues gyrating from there until it meets the green edge labelled 15. From there, it takes a safe walk to the green edge 2 which equals $k_P(e)$. Now, concatenate this with the opposite of the path going the other way, which starts at the green edge 1, follows a safe walk to green edge 14, then gyrates of length s_2 directly to green edge 2, closing the cycle. Since v_e crosses the edges e and $k_P(e)$, we find the value 1 at position 7,7 and 8,7 in the matrix for $V_{1,\theta}$. Since the gyration did a fast jump along the first blue edge, there is one more 1 in the seventh column of this matrix at position 1,7. Now, one verifies that the jumps made by the cycles v_e , for e green prongs labelled 1, ..., 13 give similar cycles described by the columns in $V_{1,\theta}$ seen below.

$$V_{1,\theta} = \left(\begin{array}{cccccc|ccccccccccccc} 1 & 0 & 0 & 0 & 0 & -1 & 1 & 0 & 0 & 0 & 0 & 0 & -1 & 0 & 0 & 0 & 0 & 0 & 0 \\ 1 & 1 & 0 & 0 & 0 & 0 & 0 & 1 & 0 & 0 & 0 & 0 & 0 & -1 & 0 & 0 & 0 & 0 & 0 \\ 0 & 1 & 1 & 0 & 0 & 0 & 0 & 0 & 1 & 0 & 0 & 0 & 0 & 0 & -1 & 0 & 0 & 0 & 0 \\ 0 & 0 & 1 & 1 & 0 & 0 & 0 & 0 & 0 & 1 & 0 & 0 & 0 & 0 & 0 & -1 & 0 & 0 & 0 \\ 0 & 0 & 0 & 1 & 1 & 0 & 0 & 0 & 0 & 0 & 1 & 0 & 0 & 0 & 0 & 0 & -1 & 0 & 0 \\ 0 & 0 & 0 & 0 & 1 & 1 & 0 & 0 & 0 & 0 & 0 & 1 & 0 & 0 & 0 & 0 & 0 & -1 & 0 \\ \hline 0 & 0 & 0 & 0 & 0 & 0 & 1 & 0 & 0 & 0 & 0 & 0 & 0 & 0 & 0 & 0 & 0 & 0 & -1 \\ 1 & 0 & 0 & 0 & 0 & 0 & 1 & 1 & 0 & 0 & 0 & 0 & 0 & 0 & 0 & 0 & 0 & 0 & 0 \\ 0 & 1 & 0 & 0 & 0 & 0 & 0 & 1 & 1 & 0 & 0 & 0 & 0 & 0 & 0 & 0 & 0 & 0 & 0 \\ 0 & 0 & 1 & 0 & 0 & 0 & 0 & 0 & 0 & 1 & 1 & 0 & 0 & 0 & 0 & 0 & 0 & 0 & 0 \\ 0 & 0 & 0 & 1 & 0 & 0 & 0 & 0 & 0 & 0 & 1 & 1 & 0 & 0 & 0 & 0 & 0 & 0 & 0 \\ 0 & 0 & 0 & 0 & 1 & 0 & 0 & 0 & 0 & 0 & 0 & 1 & 1 & 0 & 0 & 0 & 0 & 0 & 0 \\ 0 & 0 & 0 & 0 & 0 & 1 & 0 & 0 & 0 & 0 & 0 & 0 & 1 & 1 & 0 & 0 & 0 & 0 & 0 \\ 0 & 0 & 0 & 0 & 0 & 0 & 1 & 0 & 0 & 0 & 0 & 0 & 0 & 1 & 1 & 0 & 0 & 0 & 0 \\ -1 & 0 & 0 & 0 & 0 & 0 & 0 & 0 & 0 & 0 & 0 & 0 & 0 & 0 & 1 & 1 & 0 & 0 & 0 \\ 0 & -1 & 0 & 0 & 0 & 0 & 0 & 0 & 0 & 0 & 0 & 0 & 0 & 0 & 1 & 1 & 0 & 0 & 0 \\ 0 & 0 & -1 & 0 & 0 & 0 & 0 & 0 & 0 & 0 & 0 & 0 & 0 & 0 & 0 & 1 & 1 & 0 & 0 \\ 0 & 0 & 0 & -1 & 0 & 0 & 0 & 0 & 0 & 0 & 0 & 0 & 0 & 0 & 0 & 0 & 1 & 1 & 0 \\ 0 & 0 & 0 & 0 & -1 & 0 & 0 & 0 & 0 & 0 & 0 & 0 & 0 & 0 & 0 & 0 & 0 & 1 & 1 \\ 0 & 0 & 0 & 0 & 0 & -1 & 0 & 0 & 0 & 0 & 0 & 0 & 0 & 0 & 0 & 0 & 0 & 0 & 1 \end{array} \right)$$

We now choose a basis for the homology of S_θ^{inv} , as follows. Since the blue edges 1 and 2, and the green edge 1 form together a spanning tree, we can complete any other edge in the graph as a cycle in S_θ^{inv} . This way, we get a basis, and one verifies that in this basis, the monodromy is

given by the matrix

$$\left(\begin{array}{cccccccccccccccc} 0 & 1 & 0 & -1 & 0 & -1 & 1 & 0 & 0 & -1 & 1 & 0 & 0 & -1 & 1 & 0 \\ 1 & 0 & 0 & 0 & 0 & 0 & 0 & 0 & 0 & 0 & 0 & 0 & 0 & 0 & 0 & 0 \\ 0 & 1 & 0 & 0 & 0 & 0 & 0 & 0 & 0 & 0 & 0 & 0 & 0 & 0 & 0 & 0 \\ 0 & 0 & 1 & 0 & 0 & 0 & 0 & 0 & 0 & 0 & 0 & 0 & 0 & 0 & 0 & 0 \\ 0 & 0 & 0 & 0 & 1 & -1 & 1 & -1 & 1 & -1 & 1 & -1 & 1 & -1 & 1 & -1 \\ 0 & 0 & 0 & 0 & 1 & 0 & 0 & 0 & 0 & 0 & 0 & 0 & 0 & 0 & 0 & 0 \\ 0 & 0 & 0 & 0 & 0 & 1 & 0 & 0 & 0 & 0 & 0 & 0 & 0 & 0 & 0 & 0 \\ 0 & 0 & 0 & 0 & 0 & 0 & 1 & 0 & 0 & 0 & 0 & 0 & 0 & 0 & 0 & 0 \\ 0 & 0 & 0 & 0 & 0 & 0 & 0 & 1 & 0 & 0 & 0 & 0 & 0 & 0 & 0 & 0 \\ 0 & 0 & 0 & 0 & 0 & 0 & 0 & 0 & 1 & 0 & 0 & 0 & 0 & 0 & 0 & 0 \\ 0 & 0 & 0 & 0 & 0 & 0 & 0 & 0 & 0 & 1 & 0 & 0 & 0 & 0 & 0 & 0 \\ 0 & 0 & 0 & 0 & 0 & 0 & 0 & 0 & 0 & 0 & 1 & 0 & 0 & 0 & 0 & 0 \\ 0 & 0 & 0 & 0 & 0 & 0 & 0 & 0 & 0 & 0 & 0 & 1 & 0 & 0 & 0 & 0 \\ 0 & 0 & 0 & 0 & 0 & 0 & 0 & 0 & 0 & 0 & 0 & 0 & 1 & 0 & 0 & 0 \\ 0 & 0 & 0 & 0 & 0 & 0 & 0 & 0 & 0 & 0 & 0 & 0 & 0 & 1 & 0 & 0 \\ 0 & 0 & 0 & 0 & 0 & 0 & 0 & 0 & 0 & 0 & 0 & 0 & 0 & 0 & 1 & 0 \end{array} \right)$$

Correspondingly, take dual segments to any edge in the complement of the spanning tree, which form a basis. The variation map is then given by the matrix

$$\left(\begin{array}{cccccccccccccccc} 1 & 0 & 0 & 0 & 0 & -1 & 0 & 0 & 0 & 0 & 0 & 1 & 0 & 0 & 0 & 0 \\ 1 & 1 & 0 & 0 & 0 & 0 & -1 & 0 & 0 & 0 & 0 & 0 & 1 & 0 & 0 & 0 \\ 0 & 1 & 1 & 0 & 0 & 0 & 0 & -1 & 0 & 0 & 0 & 0 & 0 & 1 & 0 & 0 \\ 0 & 0 & 1 & 1 & 0 & 0 & 0 & 0 & -1 & 0 & 0 & 0 & 0 & 0 & 1 & 0 \\ 0 & 0 & 0 & 0 & 1 & 0 & 0 & 0 & 0 & 0 & 0 & 0 & 0 & 0 & 0 & 0 \\ 0 & 0 & 0 & 0 & 0 & 1 & 1 & 0 & 0 & 0 & 0 & 0 & 0 & 0 & 0 & 0 \\ -1 & 0 & 0 & 0 & 0 & 1 & 1 & 0 & 0 & 0 & 0 & 0 & 0 & 0 & 0 & 0 \\ 0 & -1 & 0 & 0 & 0 & 0 & 1 & 1 & 0 & 0 & 0 & 0 & 0 & 0 & 0 & 0 \\ 0 & 0 & -1 & 0 & 0 & 0 & 0 & 1 & 1 & 0 & 0 & 0 & 0 & 0 & 0 & 0 \\ 0 & 0 & 0 & -1 & 0 & 0 & 0 & 0 & 1 & 1 & 0 & 0 & 0 & 0 & 0 & 0 \\ 0 & 0 & 0 & 0 & 0 & 0 & 0 & 0 & 0 & 1 & 1 & 0 & 0 & 0 & 0 & 0 \\ 1 & 0 & 0 & 0 & 0 & 0 & 0 & 0 & 0 & 0 & 0 & 1 & 1 & 0 & 0 & 0 \\ 0 & 1 & 0 & 0 & 0 & 0 & 0 & 0 & 0 & 0 & 0 & 0 & 0 & 1 & 1 & 0 \\ 0 & 0 & 1 & 0 & 0 & 0 & 0 & 0 & 0 & 0 & 0 & 0 & 0 & 0 & 1 & 1 \\ 0 & 0 & 0 & 1 & 0 & 0 & 0 & 0 & 0 & 0 & 0 & 0 & 0 & 0 & 0 & 1 \end{array} \right)$$

9 Software implementation

We have implemented the algorithms described in this paper in a Python script `var_class.py` located in a Github repository. This script relies on `Singular` for resolution of singularities and `NetworkX` for graph manipulations.

9.1 Usage

To use the software, ensure you have `Singular` installed and accessible in your path. The Python dependencies are `networkx`, `matplotlib`, `numpy`, and `sympy`.

The main function is `run_polynomial(polynomial)`, which takes a polynomial string as input and returns the resolution graph and other data structures.

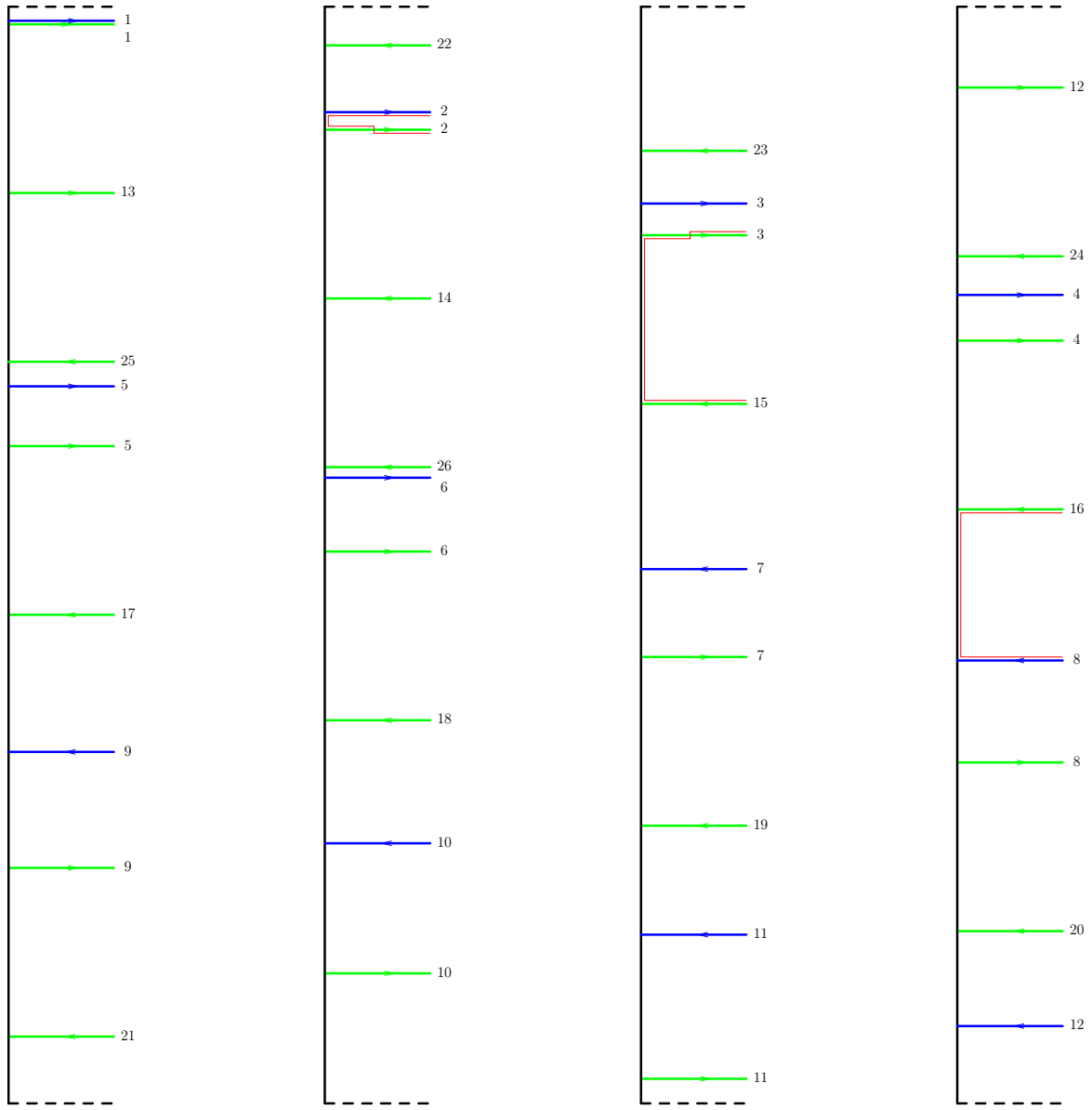


Figure 8.3.2: A blown up gyrograph for a plane curve with two Puiseux pairs. The red path is the variation map applied to a relative cycle intersecting the green segment 2 precisely once.

9.2 Example

Consider the polynomial $f(x, y) = (y^2 + x^3)(x^2 + y^3)$. We run the following code to compute the resolution graph and the algebraic invariants. We define a parameter $T = 1/100$ corresponding to the angle $\theta = 2\pi/100$. In the code we scale the angle θ by $1/2\pi$ for simplification. We compute the monodromy matrix M , the variation matrix Var , and the differential map DI on the chain complex. Then, we compute the Smith Normal Form of DI to find a basis where the differential is diagonal. This allows us to identify the homology of the complex (the kernel of DI). We denote by V the change of basis matrix. The matrices M_H and Var_H represent the restrictions of the monodromy and variation operators to the homology.

```
import var_class
import sympy as sp
from fractions import Fraction
G, H, Up, EN, mult = var_class.run_polynomial("(y^2+x^3)*(x^2+y^3)")
var_class.draw_resolution_graph(G, H, mult=False, order=False, euler=True)
```

This produces the resolution graph shown in Fig. 9.2.1.

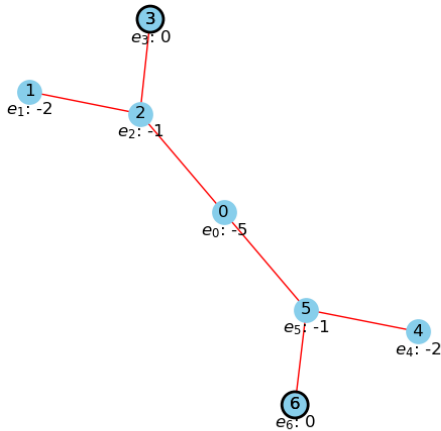


Figure 9.2.1: Resolution graph for $(y^2 + x^3)(x^2 + y^3)$ produced by the software.

```
# We define the parameters and compute the matrices
T = Fraction(1, 100)
M = var_class.monodromy_matrix(EN, G, Up, H, T)
M = sp.Matrix(M)
Var = var_class.variation_matrix(EN, G, Up, H, T)
Var = sp.Matrix(Var)
DI = var_class.differential_map(EN, G, Up, H, T)
DI = sp.Matrix(DI)

# We compute the Smith Normal Form to find the homology
D, U, W = var_class.smith_normal_form_custom(DI)
r = DI.rank()
```

```

MH = (W**(-1)*M*W)[r:,r:]
Var_H = ((W**-1)*Var*((V.transpose())**(-1)))[r:,r:]

```

The script also computes the monodromy and variation matrices, as well as their homological counterparts.

Monodromy matrix on the complex

The monodromy matrix M acting on the chain complex.

$$M = \begin{pmatrix} 0 & 0 & 0 & 1 & 0 & 0 & 0 & 0 & 0 & 0 & 0 & 0 & 0 & 0 & 0 \\ 1 & 0 & 0 & 0 & 0 & 0 & 0 & 0 & 0 & 0 & 0 & 0 & 0 & 0 & 0 \\ 0 & 1 & 0 & 0 & 0 & 0 & 0 & 0 & 1 & 0 & 0 & 0 & 0 & 0 & 1 \\ 0 & 0 & 1 & 0 & 0 & 0 & 0 & 0 & 0 & 0 & 0 & 0 & 0 & 0 & 0 \\ 0 & 0 & 0 & 0 & 0 & 0 & 0 & 0 & -1 & 0 & 0 & 0 & 0 & 0 & 0 \\ 0 & 0 & 0 & 0 & 1 & 0 & 0 & 0 & 0 & 0 & 0 & 0 & 0 & 0 & 0 \\ 0 & 0 & 0 & 0 & 0 & 1 & 0 & 0 & 0 & 0 & 0 & 0 & 0 & 0 & 0 \\ 0 & 0 & 0 & 0 & 0 & 0 & 1 & 0 & 0 & 0 & 0 & 0 & 0 & 0 & 0 \\ 0 & 0 & 0 & 0 & 0 & 0 & 0 & 1 & 0 & 0 & 0 & 0 & 0 & 0 & 0 \\ 0 & 0 & 0 & 0 & 0 & 0 & 0 & 0 & 0 & 0 & 0 & 0 & 0 & 0 & -1 \\ 0 & 0 & 0 & 0 & 0 & 0 & 0 & 0 & 0 & 1 & 0 & 0 & 0 & 0 & 0 \\ 0 & 0 & 0 & 0 & 0 & 0 & 0 & 0 & 0 & 0 & 1 & 0 & 0 & 0 & 0 \\ 0 & 0 & 0 & 0 & 0 & 0 & 0 & 0 & 0 & 0 & 0 & 1 & 0 & 0 & 0 \\ 0 & 0 & 0 & 0 & 0 & 0 & 0 & 0 & 0 & 0 & 0 & 0 & 1 & 0 & 0 \end{pmatrix}$$

Monodromy matrix after change of basis

The monodromy matrix expressed in the basis given by the Smith Normal Form.

$$W^{-1}MW = \begin{pmatrix} 0 & 1 & -1 & 0 & 0 & 0 & 0 & 0 & 0 & 0 & 0 & 0 & 0 & 0 & 0 \\ -1 & 0 & 0 & 0 & 0 & 0 & 0 & 0 & 0 & 0 & 0 & 0 & 0 & 0 & 0 \\ 0 & 0 & -1 & 0 & 0 & 0 & 0 & 0 & 0 & 0 & 0 & 0 & 0 & 0 & 0 \\ 0 & 0 & 0 & 0 & 1 & 0 & 0 & 0 & 0 & 0 & 0 & 0 & 0 & 0 & 0 \\ 1 & 0 & -1 & 1 & 0 & 0 & 1 & -1 & 1 & -1 & 1 & 0 & 0 & 0 & 0 \\ 0 & 0 & 1 & 0 & 0 & 1 & -1 & 1 & -1 & 1 & -1 & 1 & -1 & 1 & 1 \\ 0 & 0 & 0 & 0 & 0 & 1 & 0 & 0 & 0 & 0 & 0 & 0 & 0 & 0 & 0 \\ 0 & 0 & 0 & 0 & 0 & 0 & 1 & 0 & 0 & 0 & 0 & 0 & 0 & 0 & 0 \\ 0 & 0 & 0 & 0 & 0 & 0 & 0 & 1 & 0 & 0 & 0 & 0 & 0 & 0 & 0 \\ 0 & 0 & 0 & 0 & 0 & 0 & 0 & 0 & 0 & 0 & 0 & 0 & 0 & 0 & -1 \\ 0 & 0 & 0 & 0 & 0 & 0 & 0 & 0 & 0 & 0 & 1 & 0 & 0 & 0 & 0 \\ 0 & 0 & 0 & 0 & 0 & 0 & 0 & 0 & 0 & 0 & 0 & 1 & 0 & 0 & 0 \\ 0 & 0 & 0 & 0 & 0 & 0 & 0 & 0 & 0 & 0 & 0 & 0 & 1 & 0 & 0 \\ 0 & 0 & 0 & 0 & 0 & 0 & 0 & 0 & 0 & 0 & 0 & 0 & 0 & 1 & 0 \end{pmatrix}$$

Monodromy matrix in homology

The restriction of the monodromy matrix to the homology (kernel of the differential).

$$M_H = \begin{pmatrix} 0 & 1 & 0 & 0 & 0 & 0 & 0 & 0 & 0 & 0 & 0 \\ 1 & 0 & 0 & 1 & -1 & 1 & -1 & 1 & 0 & 0 & 0 \\ 0 & 0 & 1 & -1 & 1 & -1 & 1 & -1 & 1 & -1 & 1 \\ 0 & 0 & 1 & 0 & 0 & 0 & 0 & 0 & 0 & 0 & 0 \\ 0 & 0 & 0 & 1 & 0 & 0 & 0 & 0 & 0 & 0 & 0 \\ 0 & 0 & 0 & 0 & 1 & 0 & 0 & 0 & 0 & 0 & 0 \\ 0 & 0 & 0 & 0 & 0 & 1 & 0 & 0 & 0 & 0 & 0 \\ 0 & 0 & 0 & 0 & 0 & 0 & 0 & 0 & 0 & 0 & -1 \\ 0 & 0 & 0 & 0 & 0 & 0 & 1 & 0 & 0 & 0 & 0 \\ 0 & 0 & 0 & 0 & 0 & 0 & 0 & 1 & 0 & 0 & 0 \\ 0 & 0 & 0 & 0 & 0 & 0 & 0 & 0 & 1 & 0 & 0 \\ 0 & 0 & 0 & 0 & 0 & 0 & 0 & 0 & 0 & 1 & 0 \end{pmatrix}$$

Variation operator on the complex

The variation operator Var acting on the chain complex.

$$\text{Var} = \begin{pmatrix} 1 & 0 & 0 & 1 & 0 & 0 & -1 & 0 & 0 & 0 & 0 & -1 & 0 & 0 \\ 1 & 1 & 0 & 0 & 0 & 0 & 0 & -1 & 0 & 0 & 0 & 0 & -1 & 0 \\ 0 & 1 & 1 & 0 & -1 & 0 & 0 & 0 & 0 & -1 & 0 & 0 & 0 & 0 \\ 0 & 0 & 1 & 1 & 0 & -1 & 0 & 0 & 0 & 0 & -1 & 0 & 0 & 0 \\ 0 & 0 & 0 & 0 & 1 & 0 & 0 & 0 & -1 & 0 & 0 & 0 & 0 & 0 \\ 0 & 0 & -1 & 0 & 1 & 1 & 0 & 0 & 0 & 0 & 0 & 0 & 0 & 0 \\ 0 & 0 & 0 & -1 & 0 & 1 & 1 & 0 & 0 & 0 & 0 & 0 & 0 & 0 \\ -1 & 0 & 0 & 0 & 0 & 0 & 1 & 1 & 0 & 0 & 0 & 0 & 0 & 0 \\ 0 & -1 & 0 & 0 & 0 & 0 & 0 & 1 & 1 & 0 & 0 & 0 & 0 & 0 \\ 0 & 0 & 0 & 0 & 0 & 0 & 0 & 0 & 0 & 1 & 0 & 0 & 0 & -1 \\ 0 & 0 & -1 & 0 & 0 & 0 & 0 & 0 & 0 & 0 & 1 & 1 & 0 & 0 \\ 0 & 0 & 0 & -1 & 0 & 0 & 0 & 0 & 0 & 0 & 0 & 1 & 1 & 0 \\ -1 & 0 & 0 & 0 & 0 & 0 & 0 & 0 & 0 & 0 & 0 & 1 & 1 & 0 \\ 0 & -1 & 0 & 0 & 0 & 0 & 0 & 0 & 0 & 0 & 0 & 0 & 1 & 1 \end{pmatrix}$$

Variation after change of basis

The variation operator expressed in the basis given by the Smith Normal Form.

$$W^{-1}\text{Var}(W^{-1})^T = \begin{pmatrix} 0 & 0 & 0 & 0 & 0 & 0 & 0 & 0 & 0 & 0 & 0 & 0 & 0 & 0 \\ 0 & 0 & 0 & 0 & 0 & 0 & 0 & 0 & 0 & 0 & 0 & 0 & 0 & 0 \\ 0 & 0 & 0 & 0 & 0 & 0 & 0 & 0 & 0 & 0 & 0 & 0 & 0 & 0 \\ 0 & 0 & 0 & 1 & 1 & -1 & 0 & 0 & 0 & 0 & -1 & 0 & 0 & 0 \\ 0 & 0 & 0 & 0 & 1 & 0 & 0 & 0 & 0 & -1 & 0 & 0 & 0 & 0 \\ 0 & 0 & 0 & 0 & -1 & 1 & 0 & 0 & 0 & 0 & 0 & 0 & 0 & 0 \\ 0 & 0 & 0 & -1 & 0 & 1 & 1 & 0 & 0 & 0 & 0 & 0 & 0 & 0 \\ 0 & 0 & 0 & 0 & 0 & 0 & 1 & 1 & 0 & 0 & 0 & 0 & 0 & 0 \\ 0 & 0 & 0 & 0 & 0 & 0 & 0 & 0 & 1 & 0 & 0 & 0 & 0 & -1 \\ 0 & 0 & 0 & 0 & 0 & -1 & 0 & 0 & 0 & 1 & 1 & 0 & 0 & 0 \\ 0 & 0 & 0 & 0 & -1 & 0 & 0 & 0 & 0 & 1 & 1 & 0 & 0 & 0 \\ 0 & 0 & 0 & 0 & 0 & 0 & 0 & 0 & 0 & 0 & 1 & 1 & 0 & 0 \\ 0 & 0 & 0 & 0 & 0 & 0 & 0 & 0 & 0 & 0 & 0 & 1 & 1 & 0 \\ 0 & 0 & 0 & 0 & 0 & 0 & 0 & 0 & 0 & 0 & 0 & 0 & 1 & 1 \end{pmatrix}$$

Variation in homology

The restriction of the variation operator to the homology.

$$\text{Var}_H = \begin{pmatrix} 1 & 1 & -1 & 0 & 0 & 0 & 0 & -1 & 0 & 0 & 0 \\ 0 & 1 & 0 & 0 & 0 & 0 & -1 & 0 & 0 & 0 & 0 \\ 0 & -1 & 1 & 0 & 0 & 0 & 0 & 0 & 0 & 0 & 0 \\ -1 & 0 & 1 & 1 & 0 & 0 & 0 & 0 & 0 & 0 & 0 \\ 0 & 0 & 0 & 1 & 1 & 0 & 0 & 0 & 0 & 0 & 0 \\ 0 & 0 & 0 & 0 & 1 & 1 & 0 & 0 & 0 & 0 & 0 \\ 0 & 0 & 0 & 0 & 0 & 0 & 1 & 0 & 0 & 0 & -1 \\ 0 & -1 & 0 & 0 & 0 & 0 & 1 & 1 & 0 & 0 & 0 \\ -1 & 0 & 0 & 0 & 0 & 0 & 0 & 1 & 1 & 0 & 0 \\ 0 & 0 & 0 & 0 & 0 & 0 & 0 & 0 & 1 & 1 & 0 \\ 0 & 0 & 0 & 0 & 0 & 0 & 0 & 0 & 0 & 1 & 1 \end{pmatrix}$$

Verifications

One verifies, using the above results, that the identity

$$M\text{Var}^T - \text{Var} = 0$$

holds. Restricting to homology, we verify the well known identity

$$M_H\text{Var}_H^T - \text{Var}_H = 0$$

Now we consider the differential matrix DI :

$$DI = \begin{pmatrix} 0 & 1 & 0 & -1 & 1 & -1 & 0 & 0 & 1 & 0 & 0 & -1 & 1 & 0 \\ -1 & 0 & 1 & 0 & 0 & 1 & -1 & 0 & 0 & 1 & 0 & 0 & -1 & 1 \\ 0 & -1 & 0 & 1 & 0 & 0 & 1 & -1 & 0 & -1 & 1 & 0 & 0 & -1 \\ 1 & 0 & -1 & 0 & -1 & 0 & 0 & 1 & -1 & 0 & -1 & 1 & 0 & 0 \end{pmatrix}$$

and verify that monodromy takes cycles to cycles ($DI \cdot M \cdot V$). The columns corresponding to the kernel should be, and indeed are, zero:

$$DI \cdot M \cdot V = \begin{pmatrix} 0 & 1 & -1 & 0 & 0 & 0 & 0 & 0 & 0 & 0 & 0 & 0 & 0 & 0 \\ 1 & 0 & 0 & 0 & 0 & 0 & 0 & 0 & 0 & 0 & 0 & 0 & 0 & 0 \\ 0 & -1 & 0 & 0 & 0 & 0 & 0 & 0 & 0 & 0 & 0 & 0 & 0 & 0 \\ -1 & 0 & 1 & 0 & 0 & 0 & 0 & 0 & 0 & 0 & 0 & 0 & 0 & 0 \end{pmatrix}$$

References

- [A'C75a] Norbert A'Campo. La fonction zêta d'une monodromie. *Comment. Math. Helv.*, 50:233–248, 1975.
- [A'C75b] Norbert A'Campo. Le groupe de monodromie du déploiement des singularités isolées de courbes planes. I. *Math. Ann.*, 213:1–32, 1975.
- [A'C75c] Norbert A'Campo. Le groupe de monodromie du déploiement des singularités isolées de courbes planes. II. Proc. int. Congr. Math., Vancouver 1974, Vol. 1, 395–404 (1975), 1975.
- [A'C98] Norbert A'Campo. Generic immersions of curves, knots, monodromy and Gordian number. *Publ. Math., Inst. Hautes Étud. Sci.*, 88:151–169, 1998.

- [A'C99] Norbert A'Campo. Real deformations and complex topology of plane curve singularities. *Ann. Fac. Sci. Toulouse, Math.* (6), 8(1):5–23; erratum: 8, no.2, 343, 1999.
- [A'C10] Norbert A'Campo. Tête-à-tête at twists and geometric monodromy. <https://www.math.sci.hiroshima-u.ac.jp/branched/files/2010/ACampo/ttt.pdf>, 2010.
- [A'C18] Norbert A'Campo. Lagrangian spine and symplectic monodromy. 2018.
- [dBM91] Philippe du Bois and Françoise Michel. Sur la forme de Seifert des entrelacs algébriques. (On the Seifert form of algebraic links). *C. R. Acad. Sci., Paris, Sér. I*, 313(5):297–300, 1991.
- [DBM92] Philippe Du Bois and Françoise Michel. Weight filtration and integral monodromy. *Bull. Soc. Math. Fr.*, 120(2):129–167, 1992.
- [DBR07] Philippe Du Bois and Emmanuel Robin. Devissage of the Seifert form of a plane curve germ with two branches. In *Singularity theory. Proceedings of the 2005 Marseille singularity school and conference, CIRM, Marseille, France, January 24–February 25, 2005. Dedicated to Jean-Paul Brasselet on his 60th birthday*, pages 503–555. Singapore: World Scientific, 2007.
- [EN85] David Eisenbud and Walter D. Neumann. *Three-dimensional link theory and invariants of plane curve singularities.*, volume 110 of *Annals of Mathematics Studies*. Princeton University Press, 1985.
- [Gri74] Marie-Claire Grima. La monodromie rationnelle ne détermine pas la topologie d'une hypersurface complexe. Fonctions de plusieurs Variables complexes, Sem. Francois Norguet, Oct. 1970 - Dec. 1973, Lecture Note Math. 409, 580-602 (1974)., 1974.
- [GZ74] S. M. Gusein-Zade. Intersection matrices for certain singularities of functions of two variables. *Funct. Anal. Appl.*, 8:10–13, 1974.
- [Kae96] Rainer Kaenders. The Seifert form of a plane curve singularity determines its intersection multiplicities. *Indag. Math., New Ser.*, 7(2):185–197, 1996.
- [Lê88] Dũng Tráng Lê. Polyèdres évanescents et effondrements. A fête of topology, Pap. Dedic. Itiro Tamura, 293–329 (1988)., 1988.
- [LM17] Dũng Tráng Lê and Aurélio Menegon Neto. Vanishing polyhedron and collapsing map. *Math. Z.*, 286(3-4):1003–1040, 2017.
- [Mil65] John Milnor. *Lectures on the h-cobordism theorem*. Princeton University Press, Princeton, N.J., 1965. Notes by L. Siebenmann and J. Sondow.
- [MW84] Françoise Michel and Claude Weber. Une singularité isolée dont la monodromie n'admet pas de forme de Jordan sur les entiers. (An isolated singularity whose monodromy does not admit a Jordan form over the integers). *C. R. Acad. Sci., Paris, Sér. I*, 299:383–386, 1984.
- [MW86] F. Michel and C. Weber. Sur le rôle de la monodromie entière dans la topologie des singularités. *Ann. Inst. Fourier*, 36(1):183–218, 1986.
- [PS25a] Pablo Portilla Cuadrado and Baldur Sigurðsson. monodromy_var: Code repository. https://github.com/pportilla/monodromy_var, 2025. GitHub repository.
- [PS25b] Pablo Portilla Cuadrado and Baldur Sigurðsson. The total spine of the milnor fibration of a plane curve singularity. *Memoirs of the American Mathematical Society*, 2025. Accepted for publication, arXiv:2305.12555.

- [Sel73] E. Selling. Ueber die binären und ternären quadratischen Formen. *J. Reine Angew. Math.*, 77:143–229, 1873.
- [Sig25] Baldur Sigurðsson. On the Jacobian polygon and Łojasiewicz exponent of isolated complex hypersurface singularities, 2025. arXiv:2509.06150.
- [Tei77] B. Teissier. Variétés polaires. I. Invariants polaires des singularités d'hypersurfaces. *Invent. Math.*, 40(3):267–292, 1977.
- [TMW01] Lê Dũng Tráng, Hélène Maugendre, and Claude Weber. Geometry of critical loci. *J. Lond. Math. Soc., II. Ser.*, 63(3):533–552, 2001.
- [TP79] Lê Dũng Tráng and Bernard Perron. Sur la fibre de Milnor d'une singularité isolée en dimension complexe trois. *C. R. Acad. Sci., Paris, Sér. A*, 289:115–118, 1979.
- [Trá75] Lê Dũng Tráng. Topological use of polar curves. Algebraic Geom., Proc. Symp. Pure Math. 29, Arcata 1974, 507–512 (1975)., 1975.
- [Wal04] C. T. C. Wall. *Singular points of plane curves*, volume 63 of *London Mathematical Society Student Texts*. Cambridge University Press, Cambridge, 2004.